UNIVERSITY OF OKLAHOMA

GRADUATE COLLEGE

AN INVESTIGATION OF EXPERIMENTAL PARAMETERS REQUIRED TO STUDY HYDROCARBON PHASE BEHAVIOR UNDER CONSTANT VOLUME AND CONSTANT COMPOSITION CONDITIONS

A THESIS

SUBMITTED TO THE GRADUATE FACULTY

in partial fulfillment of the requirements for the

Degree of

MASTER OF SCIENCE IN NATURAL GAS ENGINEERING AND MANAGEMENT

By

ABHIJEET CHOLKAR
Norman, Oklahoma
2016

AN INVESTIGATION OF EXPERIMENTAL PARAMETERS REQUIRED TO STUDY HYDROCARBON PHASE BEHAVIOR UNDER CONSTANT VOLUME AND CONSTANT COMPOSITION CONDITIONS

A THESIS APPROVED FOR THE
MEWBOURNE SCHOOL OF PETROLEUM AND GEOLOGICAL ENGINEERING

BY

_____
Dr. Mashhad Fahes, Chair

_____
Dr. Maysam Pournik

_____
Dr. Suresh Sharma

ACKNOWLEDGEMENTS

I would like to take this opportunity to thank all those people who have assisted me to complete my thesis and graduate studies directly or in-directly.

First and foremost, I offer my sincerest gratitude to my advisor and mentor Dr. Mashhad Fahes, who believed in me and supported me throughout my research tenure. I attribute the level of my Master's degree to her knowledge, guidance and patience to accomplish my academic goal. This thesis would not have been possible without her constant motivation.

I would be failing in my duties if I do not extend my gratitude towards Dr. Suresh Sharma. I thank him for giving me opportunity to pursue my master's degree and his continuous support at every point of my graduate studies, along with being part of my thesis defense committee.

I am also grateful to have Dr. Maysam Pournik for spending his time to read this thesis and be a member of my thesis defense committee. I learned a lot from him throughout my Masters tenure.

I humbly thank my all research group members and dear friends Soham, Sumeer, Tabish, Anvit, Aman, Mounraj, Richa and Fatema for standing with me in my high and low tides and giving me a home away from home.

In the end and most importantly, I owe everything to my parents and family for their constant encouragement and blessings.

TABLE OF CONTENTS

ACKNOWLEDGEMENT……iv

TABLE OF CONTENT……v

LIST OF TABLES.....ix

LIST OF FIGURES…….xiii

ABSTRACT……xvii

CHAPTER 1: INTRODUCTION……..1

1.1 RESEARCH OBJECTIVE……..1

1.2 ORGANIZATION OF THESIS……..……2

CHAPTER 2: LITERATURE REVIEW……...3

2.1 CONVENTIONAL PVT EXPERIMENTS…….……..…….3

2.1.1 FLASH VAPORIZATION…….4

2.1.2 DIFFERENTIAL VAPORIZATION…….….6

2.1.3 CONSTANT VOLUME DEPLETION…….……7

2.2 PHASE BEHAVIOR OF HYDROCARBON…….……...8

2.2.1 PURE SUBSTANCE/ONE-COMPONENT SYSTEM..9

2.2.2 TWO-COMPONENTS OR MULTI COMPONENTS SYSTEM……....11

2.3 EQUATION OF STATES……14

2.3.1 VAN DER WAALS EQUATION OF STATE……16

2.3.2 SOAVE-REDLICH-KWONG EQUATION OF STATE……..17

2.3.3 PENG ROBINSON EQUATION OF STATE (PR 1976)……..18

2.4 SIMULATION OF PHASE BEHAVIOR IN SHALE.....19

CHAPTER 3: RESEARCH APPROACH……..31

3.1 SIMULATION INPUT/FEED…….....….31

3.1.1 SOFTWARE: CMG-WINPROP®…….....31

3.1.2 EQUATION OF STATE USED FOR SIMULATION……..……32

3.1.3 DEFINING COMPOSITION……...33

3.1.4 COMPOSITION SPECIFICATION……34

3.1.5 OUTPUT DATA GENERATED…….34

3.2 SIMULATION APPROACH AND CALCULATIONS…….36

3.2.1 APPROACH IMPLEMENTED…….……..36

3.2.2 CALCULATIONS…….……..37

3.2.3 EXCEL FILE BUILD UP……..…….……..38

CHAPTER 4: RESULTS……40

4.1 PHASE BEHAVIOR SIMULATIONS FOR VARIOUS TWO-COMPONENT HYDROCARBON SYSTEMS……..40

4.2 THE ETHANE-PENTANE SYSTEM……47

4.3 EXPERIMENTAL RESULTS……48

4.3.1 50% ETHANE – 50% PENTANE……..48

4.3.2 40% ETHANE – 60% PENTANE……..60

4.3.3 40% ETHANE – 60% PENTANE AT INITIAL PRESSURE OF 800 PSI AND INTITAL TEMPERATURE OF 350°F……70

4.3.4 40% ETHANE – 60% PENTANE AT INITIAL PRESSURE OF 600 PSI AND INTITAL TEMPERATURE OF 350°F……81

4.4 SENSITIVITY OF RESULTS TO EQUATION OF STATE CHOICE……...90

CHAPTER 5: CONCLUSION AND RECOMMENDATIONS……94

5.1 CONCLUSION……...94

5.2 RECOMMENDATIONS……95

REFERENCES……………………………………………………………..96

APPENDIX……………………………………………………………...99

LIST OF TABLES

Table 4.1: Pressure at each temperature step for 50% Ethane – 50% Butane.....41

Table 4.2: Pressure at each temperature step for 50% Ethane – 50% Hexane……...44

Table 4.3: Pressure at each temperature step for 50% Ethane – 50% Heptane……..46

Table 4.4: Z-factor of 50% Ethane – 50% Pentane system……50

Table 4.5: Vapor phase volume percent of 50% Ethane – 50% Pentane system……..51

Table 4.6: Vapor phase mol percent of 50% Ethane – 50% Pentane system……....……52

Table 4.7: Number of moles in vapor phase of 50% Ethane – 50% Pentane system……..……....……53

Table 4.8: Vapor phase volume of50% Ethane – 50% Pentane system……....54

Table 4.9: $P*v_g/Z*n_g$ chart of 50% Ethane – 50% Pentane system……55

Table 4.10: Pressure at each temperature step for 50% Ethane – 50% Pentane system…….....57

Table 4.11: Z-factor of 40% Ethane – 60% Pentane system…….……..……..61

Table 4.12: Vapor phase volume percent of 40% Ethane – 60% Pentane system……..62

Table 4.13: Vapor phase mol percent of 40% Ethane – 60% Pentane system……63

Table 4.14: Number of moles in vapor phase of 40% Ethane – 60% Pentane system……..64

Table 4.15: Vapor phase volume of 40% Ethane – 60% Pentane system……65

Table 4.16: $P*v_g/Z*n_g$ chart of 40% Ethane – 60% Pentane system……...…….……66

Table 4.17: Pressure at each temperature step for 40% Ethane – 60% Pentane system…….....68

Table 4.18: Pressure at each temperature step for 40% Ethane – 60% Pentane system at initial pressure of 800psi.....71

Table 4.19: Z-factore of 40% Ethane – 60% Pentane system at initial pressure of 800 psi….……..…74

Table 4.20: Vapor phase volume percent of 40% Ethane – 60% Pentane system at initial pressure of 800 psi……75

Table 4.21: Vapor phase mole percent of 40% Ethane – 60% Pentane system at initial pressure of 800 psi…….……76

Table 4.22: Number of mole in vapor phase of 40% Ethane – 60% Pentane system at initial pressure of 800 psi…….……77

Table 4.23: Vapor phase volume of 40% Ethane – 60% Pentane system at initial pressure of 800 psi…….……..……78

Table 4.24: $P*v_g/Z*n_g$ chart of 40% Ethane – 60% Pentane system at initial pressure of 800 psi……...79

Table 4.25: Pressure at each temperature step for 40% Ethane – 60% Pentane system at initial pressure of 600 psi……..…81

Table 4.26: Z-factor of 40% Ethane – 60% Pentane system at initial pressure of 600 psi…….84

Table 4.27: Vapor phase volume percent of 40% Ethane – 60% Pentane system at initial pressure of 600 psi…….85

Table 4.28: Vapor phase mole percent of 40% Ethane – 60% Pentane system at initial pressure of 600 psi…….86

Table 4.29: Number of mole in vapor phase of 40% Ethane – 60% Pentane system at initial pressure of 600 psi…….87

Table 4.30: Vapor phase volume of 40% Ethane – 60% Pentane system at initial pressure of 600 psi…….....88

Table 4.31: P^*v_g/Z^*n_g chart of 40% Ethane – 60% Pentane system at initial pressure of 600 psi……...89

Table 4.32: Pressure at each temperature step for 40% Ethane – 60% Pentane using SRK equation of state…….....91

LIST OF FIGURES

Figure 2.1: Laboratory Flash Vaporization Procedure……05

Figure 2.2: Laboratory Differential Vaporization Procedure……..07

Figure 2.3: Pure substance phase diagram…….…10

Figure 2.4: Two component phase diagram……12

Figure 2.5: Phase diagram of multicomponent mixture….……13

Figure 2.6: Shifts in phase envelope of the gas mixture in bulk state and when confined to pores of 3nm and 2nm widths...22

Figure 2.7: Phase envelopes for C1(30 mol%)-nC4(35 mol%)-nC8 (35 mol%) mixtures at different pore radius (Method 1)……..24

Figure 2.8: Phase envelopes for C1(30 mol%)-nC4(35 mol%)-nC8 (35 mol%) mixtures at different pore radius (Method 2)……..25

Figure 2.9: Phase envelopes for C1(10 mol%)-nC4(25 mol%)-nC8 (65 mol%) mixtures at different pore radius (Method 2)…….……..……...26

Figure 2.10: Phase envelopes with and without capillary pressure for binary mixtures (70:30 C_1/C_4 and 70:30 C_1/C_6) and pore radius of 10 nm…….28

Figure 2.11: Phase envelopes for various C_1/C_6 mixtures and pore radius of 20 nm.....29

Figure 2.12: Temperature and pressure points within the two-phase region for the 70:30 C1/C6 mixture.…….30

Figure 4.1: Two phase diagram of 50% Ethane – 50% Butane….41

Figure 4.2: Two phase diagram of 50% Ethane – 50% Butane with superimposed Pressure versus Temperature plot……42

Figure 4.3: Two phase diagram of 50% Ethane – 50% Hexane.....43

Figure 4.4: Two phase diagram of 50% Ethane – 50% Hexane with superimposed Pressure versus Temperature plot……45

Figure 4.5: Two phase diagram of 50% Ethane – 50% Heptane....46

Figure 4.6: Two phase diagram of 50% Ethane – 50% Heptane with superimposed Pressure versus Temperature plot...….47

Figure 4.7: Two-phase diagram of 50%Ethane – 50% Pentane....49

Figure 4.8: P^*v_g/Z^*n_g versus Pressure of 50% Ethane – 50% Pentane……56

Figure 4.9: Pressure versus temperature of 50% Ethane – 50% Pentane…….58

Figure 4.10: Two phase diagram of 50% Ethane – 50% Pentane with superimposed Pressure versus Temperature plot……...59

Figure 4.11: Two-phase diagram of 50% Ethane – 50% Pentane.….60

Figure 4.12: P^*v_g/Z^*n_g versus Pressure of 50% Ethane – 60% Pentane…….…67

Figure 4.13: Pressure versus Temperature of 40% Ethane – 60% Pentane…….……69

Figure 4.14: Two phase diagram of 40% Ethane – 60% Pentane with superimposed Pressure versus Temperature plot…...…70

Figure 4.15: Pressure versus Temperature 40% Ethane – 60% Pentane…….…….....72

Figure 4.16: Two phase diagram of 40% Ethane – 60% Pentane at initial pressure of 800 psi with superimposed Pressure versus Temperature plot…….…...…..……73

Figure 4.17: P^*v_g/Z^*n_g versus Pressure of 40% Ethane – 60% Pentane at initial pressure of 800 psi……80

Figure 4.18: Pressure versus Temperature of 40% Ethane – 60% Pentane at initial pressure of 600 psi……82

Figure 4.19: Two-phase diagram of 40% Ethane – 60% Pentane at initial pressure of 600psi with superimposed Pressure versus Temperature plot…….……...…...83

Figure 4.20: P^*v_g/Z^*n_g versus Pressure of 40% Ethane – 60% Pentane at initial pressure of 600 psi……90

Figure 4.21: Two-phase diagram of 40% Ethane – 60% Pentane using SRK equation of state…….……91

Figure 4.22: Pressure versus temperature of 40% Ethane – 60% Pentane using SRK equation of state……92

Figure 4.23: Two-phase diagram of 40% Ethane – 60% Pentane superimposed pressure versus temperature plot using SRK and PR equation of states…….93

ABSTRACT

Accurate fluid phase behavior evaluation is essential for reservoir engineers to predict the type of reservoir, oil and gas in place, and develop proper production strategies. The change in phase behavior and phase equilibrium are key to understand the reservoir condition and estimate production from a particular formation. In shale reservoirs, hydrocarbon phase behavior in nanopores can be affected by various factors such as pore proximity and pore size distribution. In many shale and tight oil and gas reservoirs, pore sizes are in the ranges of nanometers.

Various simulation models are seen in literature attempting to predict phase behavior under confinement but there is no good reference of experimental results for verification. Our research team is trying to conduct phase behavior tests for single, binary, and multi-component hydrocarbon mixtures under confinement to validate and test the various simulation models. Since that's not an easy endeavor, each of us in the research team has taken on one of the challenging tasks to accomplish the goal. My particular goal is to examine the feasibility of a new experimental procedure for detecting the edge of the phase envelope.

The new experimental approach for detecting the phase envelope was examined through numerical simulation of binary hydrocarbon mixtures in bulk since these bulk simulation numbers have been verified experimentally in the past.

The binary hydrocarbon mixtures we examined were Ethane with Propane, Pentane, Heptane and Hexane with 50-50 mole percentage. As per the experimental feasibility in the laboratory and lower temperature and pressure ranges available, various compositions of Ethane-Pentane system were studied in order to design the experimental parameters. The results of this study will be used by the rest of the members in the research team to conduct the experiments as it provided them with the most suitable system to explore in the laboratory.

CHAPTER 1: INTRODUCTION

1.1 RESEARCH OBJECTIVE

For designing optimum recovery processes and enhancing hydrocarbon production from an oil and gas reservoir, reliable measurement and prediction of phase behavior and properties of petroleum reservoir fluids are important. Development of experimental and simulation methods to calculate and determine petroleum reservoir fluid properties along with oil and gas recovery techniques, requires to emphasize on Pressure-Volume-Temperature and phase behavior data of a reservoir. To get reliable results of physical properties and phase behavior simulations, it is highly important to get accurate fluid compositions and PVT data. Phase behavior of a mixture with known composition consists of the number of phases, phase compositions, phase amounts, as well as phase properties such as molecular weight, density and viscosity.

The determination of phase change of a reservoir fluid or the phase behavior of the hydrocarbon mixture in an oil and gas reservoir depends upon various factors and conditions within the reservoir such as pore size distribution, pore proximity effect, capillary pressure as well as varying pressure and temperature conditions. In particular, shale gas reservoirs are an example of such reservoirs that are highly affected by these factors.

In this study, the objective was to examine the feasibility of phase change detection using an experimental procedure that would be suitable for implementation under nano-pore confinement conditions.

1.2 ORGANIZATION OF THESIS

The research study conducted has been divided into 5 chapters.

Chapter 1 covers the introduction and the objective to carry out research in this topic.

Chapter 2 covers the background and literature review for the study which includes understanding the phase behavior in shale and the simulation approach used by others so far.

Chapter 3 focuses on the way software was used in our study for bulk simulation and how data was generated. The focus is the research approach implemented to determine the parameters required for future experimental studies of phase behavior under confinement.

Chapter 4 includes the results of bulk phase behavior simulation for various two-component hydrocarbon systems. It also focuses on choice of ethane-pentane system based on experimental feasibility and various initial pressure options used for the system.

Chapter 5 summarizes the major conclusions of the study and recommendation for future work.

CHAPTER 2: LITERATURE REVIEW

The literature review is organized along the following lines. We first review the conventional PVT experiments commonly conducted in laboratories, we then review the common trends in hydrocarbon phase behavior, we discuss the equations of state commonly used to represent this behavior, and at the end we present the detailed review of the various simulation studies that attempt to represent the effect of confinement on phase behavior.

2.1 CONVENTIONAL PVT EXPERIMENTS

Conventional PVT tests are commonly conducted in the laboratory by placing the mixture under investigation in a PVT cell with a typical volume of around 100 cc. The results from this cell represent bulk phase behavior since the fluids are not exposed to confinement. A list of such tests include:

- Compositional Measurement.
- Flash Vaporization also termed as Constant Composition Expansion
- Differential Vaporization
- Constant Volume Depletion
- Separator Test.
- Viscosity Measurements.

Below we review the experimental details associated with 3 of these tests, namely Flash Vaporization, differential vaporization and constant volume depletion.

2.1.1 FLASH VAPORIZATION

This experimental procedure is also known as Constant Composition Expansion (CCE), Pressure Volume Relations, Flash Liberation or Flash Vaporization (McCain, 1990). In this experiment, a known mass of reservoir fluid is placed in a laboratory cell and the thermal environment is maintained constant at reservoir temperature throughout the experiment. Theoretically, the pressure condition set should be approximately that of initial reservoir pressure. However, for the experimental purpose, the sample is initially brought to a pressure slightly above the initial reservoir pressure. As the pressure is reduced, the oil volume increases or the oil expands. (McCain, 1990)

Throughout the experiment, periodic agitation of the fluid is carried out to ensure the equilibrium of the contents. Agitation prevents the phenomenon of supersaturation, or metastable equilibrium, where a mixture remains as a single phase even though it should exist as two phases (McCain, 1990). By agitating the mixture at each new pressure, the condition of supersaturation is prevented, allowing more accurate determination of the bubble point. Meanwhile, no reservoir liquid or gas is removed from the cell. Pressure and volume of the fluid in the cell is measured during each step and the total volume is termed as total volume V_t.

When the obtained P-V plot is studied, the pressure at which the slope changes is the bubble point pressure of the mixture at the given temperature. The corresponding volume at the bubble point is the saturated volume of the liquid

which is represented by the symbol V_{sat}. The volume of the liquid at bubble point can be divided by the mass of reservoir fluid in the cell to obtain a value of specific volume at the bubble point. Specific volume at the bubble point is also measured during other tests and is used as a quality check for the data.

All values of total volume V_t, are divided by volume at the bubble point and the data are reported as relative volumes. Sometimes the symbol V/V_{sat} is used, however, this document denotes the same by the symbol $(V_t/V_b)_F$. The symbol $(V_t/V_b)_F$ indicates the ratio of total volume and volume at the bubble point during a flash vaporization process. (McCain, 1990)

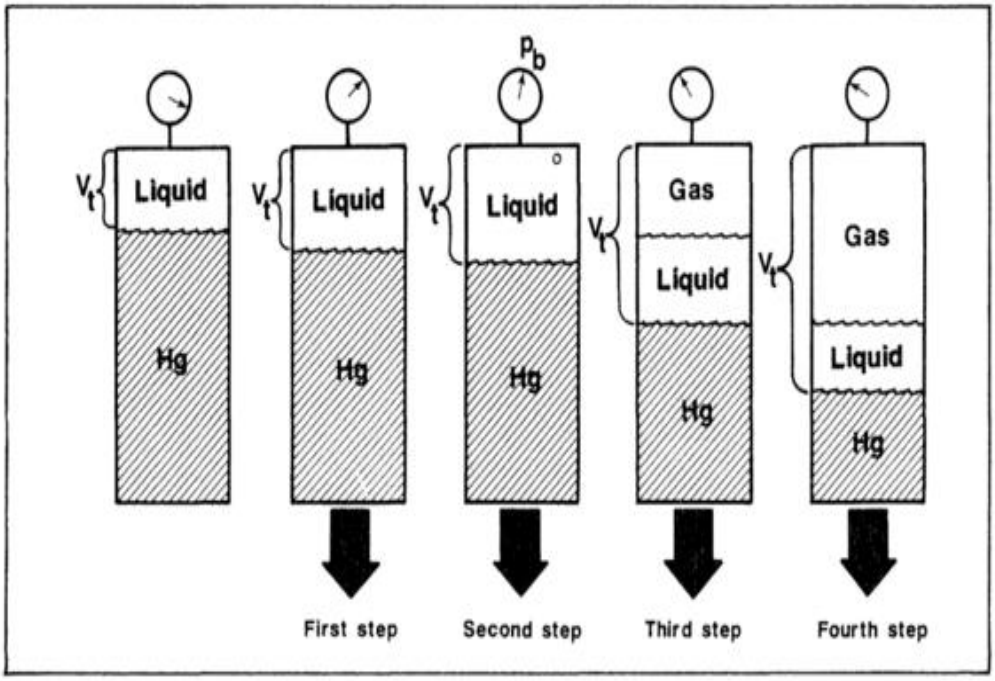

Figure 2.1: Laboratory flash vaporization procedure (McCain, 1990)

2.1.2 DIFFERENTIAL VAPORIZATION

The Differential Vaporization or Differential Liberation experiment is designed to approximate the depletion process of an oil reservoir and to provide suitable PVT data in order to calculate the reservoir performance.

The sample of reservoir fluid in the laboratory cell is conditioned to a single phase at reservoir temperature. Pressure is reduced by increasing cell volume until the fluid reaches its bubble point. The cell is then agitated to ensure equilibrium between the gas and liquid. Since the initial mass of the sample is known, bubble point density can be calculated. Next, all the gas is expelled from the cell while maintaining a constant pressure in the cell by reducing cell volume.

The gas is collected, and its volume, amount (in moles) and specific gravity are measured. The volume of liquid remaining in the cell, V_o is measured. The process is repeated in steps until atmospheric pressure is reached. The temperature is then reduced to 60 °F, and the residual oil (the remaining oil in the cell) volume and its specific gravity is measured. This process is either called differential vaporization, differential liberation, or differential expansion. Each of the values of cell liquid volume V_o, is divided by the volume of the residual oil. The resultant defined as relative oil volume is denoted by the symbol B_oD. (McCain, 1990)

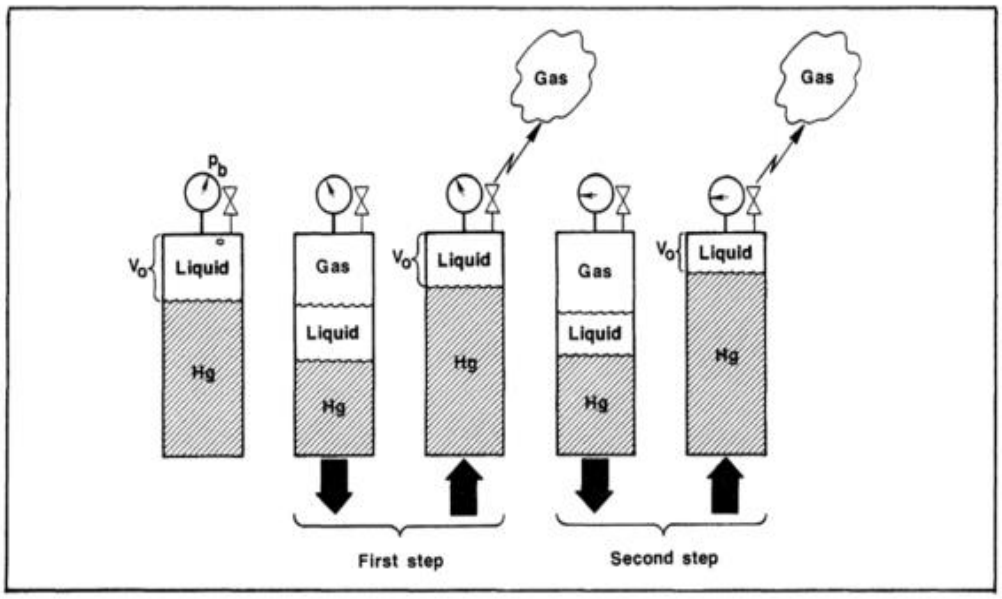

Figure 2.2: Laboratory differential vaporization procedure (McCain, 1990)

2.1.3 CONSTANT VOLUME DEPLETION

The CVD experiment is designed to provide the volumetric and compositional data for gas-condensate reservoirs producing due to pressure depletion. These experiments provide data that can be used directly by the reservoir engineer, including (1) a reservoir material balance that provides average reservoir pressure vs. recovery of total well stream (wet-gas recovery), sales gas, condensate, and natural gas liquids; (2) produced well stream composition and surface composition at given reservoir pressure; and (3) average oil saturation in the reservoir (liquid dropout and re-vaporization) that occurs during pressure depletion.

In CVD experiment for gas-condensate reservoir, the pressure and temperature conditions of the test cell are initially set to that representing the dew point or bubble point condition of the reservoir fluid, and recorded. Next, the pressure is reduced, usually by small amounts (50 to 250 psi), just below the saturation pressure of more volatile systems. The cell is agitated until equilibrium is achieved and volumes V_o and V_g are measured. At a constant pressure, sufficient volume of gas ΔVg is removed to return the cell volume to the original saturated volume.

The removed gas is brought to atmospheric conditions, where the amount of surface gas and condensate is measured. Produced surface volumes from the reservoir gas are measured and other parameters such as densities and oil molecular weights are measured as well.

2.2 PHASE BEHAVIOR OF HYDROCARBONS

Phase is defined as any homogeneous and physically distinct part of a system which is separated from other parts of the system by definite boundaries. A system may be classified as a one, two, or multicomponent system. For example, an oil reservoir (liquid phase) during depletion may form gas (vapor phase) which could remain dispersed in oil as a mixture before forming a mobile cluster (gas). However, both the cases can be considered as a two-phase system (Sherborne, 1940) [1].

2.2.1 PURE SUBSTANCE/ONE-COMPONENT SYSTEM

These kind of system consist of only single, pure substance. These systems behave differently from systems which are made up of two or more components. The phase behavior of a pure substance is shown in form of a pressure-temperature diagram in Fig. 2.3. The plots of pressure against temperature exhibiting the conditions under which the various phases of the substance exist are known as phase diagrams or pressure-temperature diagrams (McCain, 1990) [2]. Below are a few definitions of the characteristics of such diagrams.

Bubble Point Pressure: In its original condition, reservoir fluid includes some amount of natural gas dissolved in it. The pressure at which this natural gas begins to emerge out of the solution and form bubbles is known as the bubble-point pressure.

Dew Point Pressure: At a certain temperature at which fluid begins to condense from the vapor phase in a gas stream when pressure is decreased below the bubble point pressure, is called dew point pressure.

Critical Point: For a pure substance, critical point is the upper limit of the vapor-pressure line (indicated by point C here) and the pressure and temperature represented by this point are called as the critical pressure P_c and the critical temperature T_c respectively.

For a pure substance, the critical pressure is defined as the pressure above which liquid and gas cannot co-exist, regardless of the temperature. Similarly, the

critical temperature is defined as the temperature above which gas cannot be liquefied (McCain, 1990) [2].

Vapor-pressure line: The vapor-pressure line or vaporization/saturation curve represents the locus of points where the liquid and vapor phases are in equilibrium. Lines A-C represent the above discussed vapor-pressure line in the Fig. 2.3.

This line demarcates the pressure-temperature conditions for which the substance is a liquid from the conditions for which the substance is a gas. For a substance said to be liquid, the pressure-temperature points should lie above this line. Similarly, for a substance said to be gas, the pressure-temperature points should lie below this line. The pressure-temperature points which lie exactly on the line indicate the condition for liquid and gas to coexist.

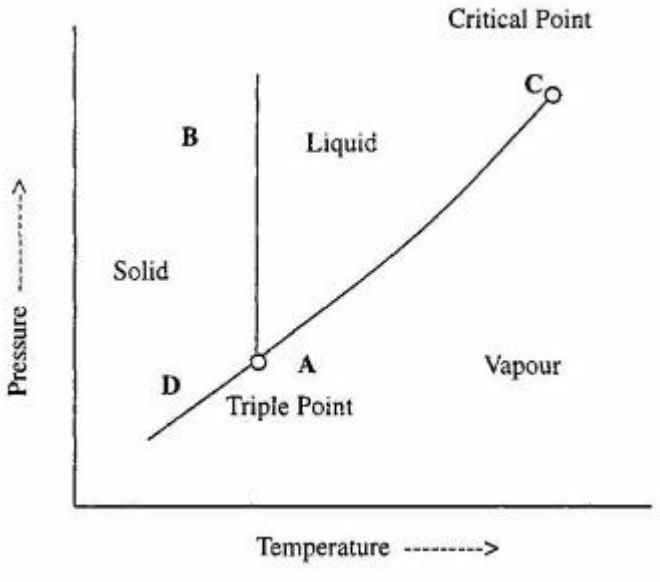

Figure 2.3: Pure substance phase diagram (Danesh, 1998)

Triple point: The point on phase diagram which represents the temperature and pressure at which solid, liquid and gas phase coexist under equilibrium conditions, is known as Triple point.

Sublimation-pressure line or Sublimation curve: It is the locus of points where solid and vapor phases are in equilibrium. At temperatures below the triple-point temperature, the vapor pressure line separates the conditions for which the substance is solid from the conditions for which the substance is gas (McCain, 1990)[2].

Melting point line or fusion curve: It is the locus of points where solid and liquid are in equilibrium. This line separates solid conditions from liquid conditions. It is nearly vertical to the triple point and in upward direction. The pressure and temperature points which fall exactly on this line indicate a two phase system. In this case, it depicts the coexistence of solid and liquid phase.

2.2.2 TWO-COMPONENTS OR MULTI-COMPONENTS SYSTEM

The phase behavior of a mixture of two components or multi-component system is more elaborate than that of a pure component. The reservoir fluids are mainly composed of hydrocarbons with widely different molecular structures and sizes. Therefore, their phase behavior is highly complex.

For a binary system, the phase behavior is relatively simpler and is very much similar to a real multi-component reservoir fluid. In comparison to a single-component system, instead of using a single line to represent the vapor-pressure

curve, a broad region is used for a two-component system in which two phases coexist (Fig. 2.4). This region is known as either the phase envelope, saturation envelope or the two-phase region.

The two phase region of the phase envelope, inside which the two phases coexist is bounded by the bubble-point curve on one side and by the dew-point curve on the other. The two curves/lines meet at the critical-point(C), where the phases become indistinguishable. The critical pressure of a two-component mixture usually will be higher than the critical pressure of either of the components and the critical temperature of the mixture lies between the critical temperatures of the two pure components. (Danesh, 1998)

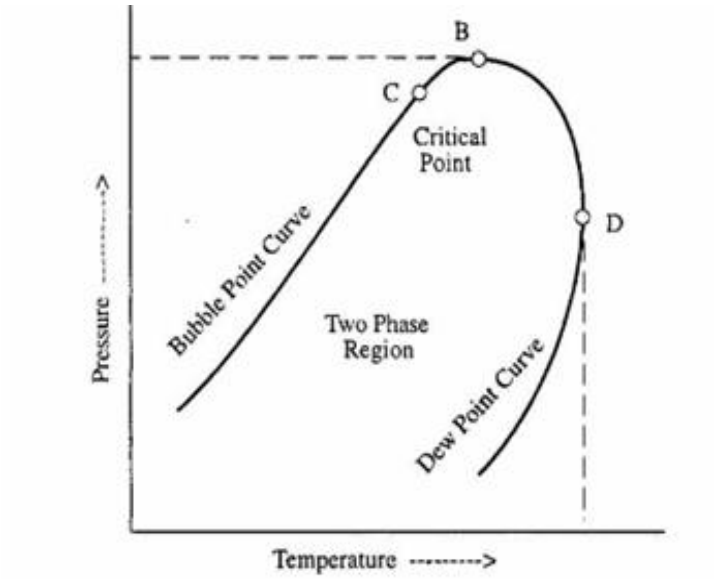

Figure 2.4: Two component phase diagram (Danesh, 1998)

The highest temperature on the phase envelope is called as the cricondentherm and the highest pressure on the phase envelope is called as the cricondenbar.

Retrograde Condensation

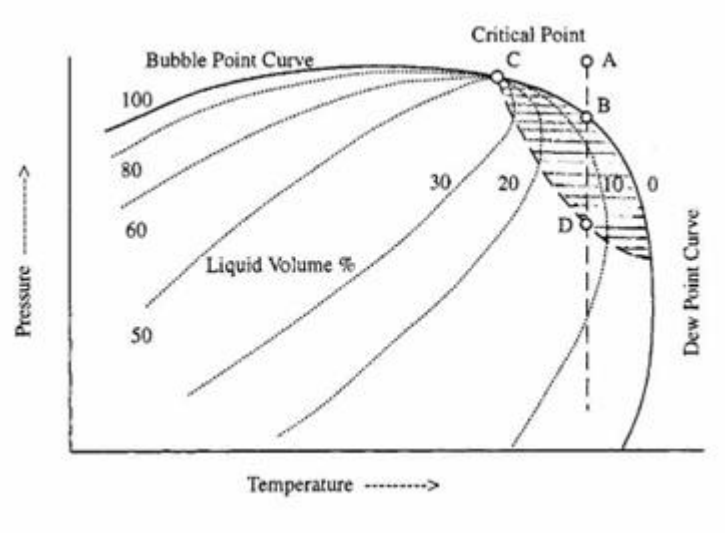

Figure 2.5: Phase diagram of a multicomponent mixture (Danesh, 1998)

For a pure substance, reduction in pressure at constant temperature causes change of phase from liquid to gas at the vapor-pressure line. Similarly, in case of two-component system a small reduction in pressure or temperature at a region near the critical point cause major phase change (from liquid to gas).

Consider isothermal reduction of pressure illustrated by line ABD in Fig.2.5 for a vapor-like fluid from point A. As the dew point line is crossed the first drop of liquid is seen at point B. The fluid in the shaded region of the phase diagram exists as both, liquid and gas. Further pressure reduction results in condensation and the state of the fluid now lies in what is termed as retrograde region. Hence, further reduction in pressure from Point B will result in condensation and this phenomenon is called retrograde condensation. The condensation will stop at some point D, and the condensed phase of the fluid will re-vaporize after further

reduction in pressure. This behavior of phase change is exactly the reverse of the behavior that would be expected; hence, the name retrograde condensation. Retrograde condition occurs only if the gas temperature lies between the critical temperature and the cricondentherm. There are two dew point pressures that exist at any temperature for retrograde gases – upper dew point and lower dew point. The upper dew point is also called the retrograde dew point (Danesh, 1998). A similar retrograde situation occurs when temperature is changed at constant pressure between the critical pressure and cricondenbar.

2.3 EQUATIONS OF STATE

An equation of state is an analytical expression which is widely used to determine and/or calculate the thermodynamic properties, volumetric behavior, and vapor – liquid equilibria (VLE) or phase equilibria of pure components and (their) mixtures. This expression relates the pressure to the volume and temperature. For the design and optimization of various processes in different industrial segments such as chemical industries and oil and gas, the accurate knowledge of these properties over a wide range of pressure, temperature and composition is critical.

Cubic equations of state (EOS) are the most popular class of equations of state which originated from 'Van der Waals' equation of state which he introduced in 1873. This equation of state was the first thermodynamic model applicable to both pure oil and gas state of fluids. Numerous equations of state were proposed since Van der Waals equation of state was introduced. These equations were

then modified for mixtures incorporating the mixing rules in consideration and extended for range of pressure and temperatures to include subcritical, near critical and supercritical conditions. The extensions and modifications were also based on the fluids that are of variable molecular size such as small spherical molecule to long-chain molecules. Along with these changes, some models have been extended for multicomponent mixtures that could be of same or different molecular shape and size (Sengers, 2010)[4].

Ideal gas equation

The simplest and most fundamental EOS is the ideal gas equation, in which the variables pressure, volume, and temperature of a fluid are related by

$$pV = RT. \tag{1}$$

As stated previously, the behavior of a gas may be approximated by Eq. 1 if the pressure is relatively low. A gas is ideal if molecular interactions are negligible, something that could only occur at zero pressure. Thus, molecular interactions are negligible at zero pressure; therefore, thermodynamic properties, such as the molar internal energy of an ideal gas, are only a function of temperature. (McCain, 1990)

2.3.1 VAN DER WAALS EQUATION OF STATE

The ideal gas equation was improved by van der Waal in which he considered intermolecular attractive and repulsive forces. According to van der Waals EOS, the temperature T, pressure P and molar volume V_m of a fluid are interrelated according to expression:

$$P = \frac{RT}{Vm-b} - \frac{a}{Vm^2} \qquad \text{eq. (2.1)}$$

Where, R is the gas constant, a and b represents attraction and repulsion parameters respectively. Sometimes the molar volume becomes equal to 'b' when the pressure approaches infinite. Thus, b is called the co-volume as it is considered as an apparent volume of the molecule.

Re-writing the van der Waals equation of state in a polynomial form results in a third-order (cubic) equation with respect to volume. These equations of state are often referred to as cubic equation of state.

When real fluids are considered for engineering applications, the parameters a and b are calculated by imposing the critical-point conditions to the equation of state, given as:

$$\left(\frac{\partial P}{\partial Vm}\right)Tc = \left(\frac{\partial^2 P}{\partial V_m^2}\right) = 0$$

The values of a and b are determined as:

$$a = \frac{27\ R^2(T_C)^2}{64 \quad Pc} \qquad \text{eq. (2.2)}$$

And,

$$b = \frac{RT_C}{8P_C} \qquad \text{eq. (2.3)}$$

Where, the subscript *c* refers to the values at critical point. Equations 2.1, 2.2 and 2.3 provide a qualitative description of vapor-liquid equilibrium (VLE) and PVT properties of real fluids (either oil or gas) such as argon or methane. Thus it cannot accurately model the behavior of dense fluids, particularly, that of the complex fluids mixtures. This inefficiency of the model led to the numerous additions and modifications in the van der Waals equation of state.

2.3.2 SOAVE-REDLICH-KWONG EQAUTION OF STATE (SRK)

Soave proposed a significant improvement to the Redlich-Kwong equation of state by replacing the temperature dependency of the attraction term by a more general function α. This parameter is also a function of the acentric factor ω. The Redlich-Kwong EOS is written as:

$$P = \frac{RT}{V_m - b} - \frac{a\alpha}{V_m(V_m + b)}$$

Where,

$$\alpha = \frac{1}{T^{0.5}}$$

$$a = \Omega_a \left(\frac{R^2 (T_C)^{2.5}}{P_C} \right) = 0.42748 \left(\frac{R^2 (T_C)^{2.5}}{P_C} \right)$$

$$b = \Omega_b \frac{RT_C}{P_C} = 0.08664 \frac{RT_C}{P_C}$$

And,

$$\alpha = [1 + (1 - T_r^{0.5})(0.480 + 1.574\omega - 0.176\omega^2)]^2,$$

Where $T_r = T/T_c$. This new cubic equation of state showed a significant improvement over Redlich-Kwong for pure hydrocarbons as well as for hydrocarbon mixture VLE. SRK is quite capable of predicting VLE but it does not provide reliable liquid density.

2.3.3 PENG ROBINSON EQUATION OF STATE (PR 1976)

Peng-Robinson modified the denominator of the attraction term and used a different expression and functional form for the parameters a and b in order to improve the prediction of liquid density in comparison with SRK.

$$P = \frac{RT}{V_m - b} - \frac{a\alpha}{V_m(V_m + b) + b(V_m - b)}$$

Where,

$$a = 0.42748\left(\frac{R^2(T_C)^2}{P_C}\right)$$

$$\alpha = [1 + (1 - T_r^{0.5})(0.37464 + 1.54226\omega - 0.26992\omega^2)]^2,$$

And,

$$b = 0.07780\frac{RT_C}{P_C}.$$

Peng-Robinson and Soave-Redlich-Kwong equations of state are widely used and currently, are the most popular cubic equations of state. They are used to calculate the properties of pure component, single phase primary and derivative properties, and more importantly properties of multicomponent mixtures including both low and high pressure VLE and liquid-liquid equilibrium (LLE).

2.4 SIMULATION OF PHASE BEHAVIOR IN SHALE

Many researchers have previously carried out modeling studies on phase behavior in shale with various models such as using different pore sizes, pore size distributions, varying gas composition (e.g. primary, binary and ternary mixture), and studying phase behavior dependency on capillary pressure, etc.

Phase behavior and fluid properties of the hydrocarbons could be influenced by the nano-porous nature of the rocks and are governed by molecule-molecule and molecule-pore wall interactions.

Akkutlu et al. (2013) used Monte Carlo simulation to find out the pure hydrocarbon vapor-liquid coexistence and critical properties under confinement. The model was used to study adsorption of gases in laboratory fabricated nano-pores using different temperatures, pressures and pore sizes. The study exhibits the dependence of these thermo-physical properties on pore size and shift of the two-phase envelop due to pore size. Ternary mixtures (C_1, C_4, and C_8) were used for generating the phase diagram. Moreover, binary gas mixtures were also studied. It was concluded that the thermo-physical properties of fluids differ from their bulk values for the fluids under confinement (Gelb et at., 1999).

As a result of Monte Carlo simulations done by Akkutlu et al. (2013) to investigate pure hydrocarbon vapor-liquid coexistence and critical properties under confinement, it showed a pore size dependence of these thermos-physical properties. There was a two-phase envelop shift due to pore size dependence as phase diagram was generated using a ternary mixtures under reservoir conditions. It was found out that, the liquid production from the gas condensate shales can be improved significantly by controlling the bottom-hole production pressures. It is possible to attain more liquid production from shale reservoirs with nano-pores because of shift in the phase envelop.

When thermodynamic equilibrium simulation at high pressure and temperature reservoir condition was carried out for single hydrocarbon or primary mixture i.e. methane; it was found out that methane cannot be considered as free gas. This is attributed to the reason that methane acts like a dissolved gas at high pressure even in the large pores because its density in the center of the pore is much higher than the bulk density. With these simulations it can be seen that the thermodynamic state of the fluid under confinement really depends not only on the pressure and temperature but also on the pore size.

Akkutlu et al. (2009) employed CMG calculations to compare the production of a gas mixture, under confinement conditions and in bulk conditions for the pore sizes of 3nm and 2nm pores (Figure 2.6). This resulted into phase diagram from smaller pores to lower critical temperature and pressures, putting the initial reservoir condition in higher supercritical states, hence delaying the reaching to dew point line.

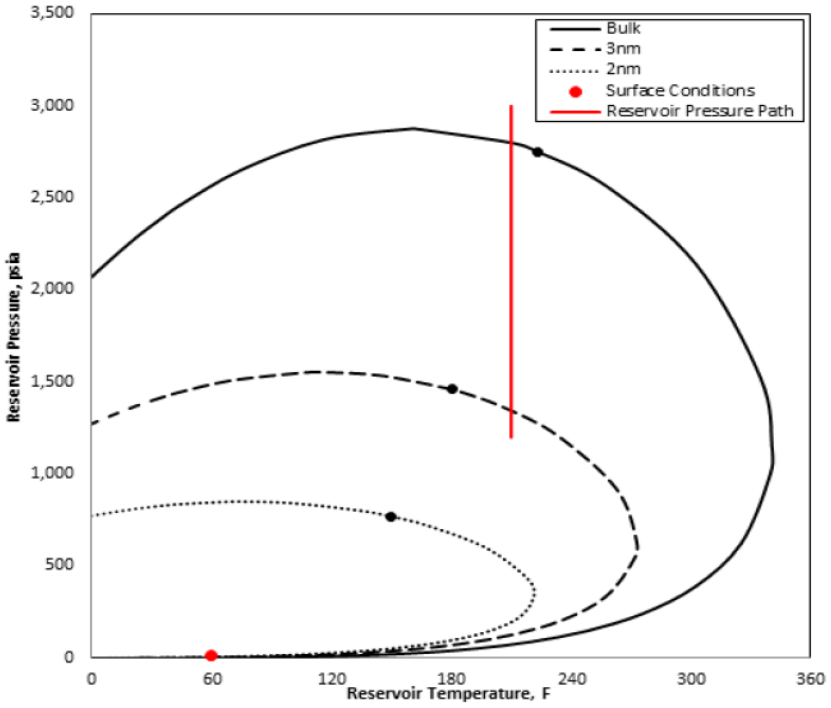

Figure 2.6: Shifts in phase envelopes of the gas mixture in bulk state when confined to pores of 3nm and 2nm widths. Black dots and red solid line represent the critical points and the production path, respectively. (Akkutlu et al., 2009)

Jin et al. (2013) conducted simulation to study the effect of pore proximity on phase behavior and fluid properties in shale formations. The investigation was primarily based on two methods developed during initial study. First, a new flash calculation algorithm considering the effect of capillary pressure on phase behavior was proposed. Second, the effect of pore size on critical properties of each component was taken into account to develop a new correlation based on molecular simulation studies.

The research involved simulations on the phase behavior and fluid properties of a mixture of Methane, n-Butane and n-Octane, with different compositions, under confinement for pore size range from infinite to 2nm by using both the methods. The first method yields in a significant shrinkage of the two phase envelope as compared to the second method with decreasing pore size. It was also determined that the effect of pore size on two phase envelope becomes significant when pore radius is smaller than 10 nm. This conclusion was in agreement with Sigmund et al. (1973) who studied the theoretical and experimental effects of pore size on phase behavior by including capillary pressure term in flash calculations. Sigmund et al. (1973) used a binary mixture system of Methane and n-Pentane for their study. It was found that the decrease in the bubble point pressures and changes in vapor compositions are very small for pore radius more than 100nm. Although, these results provide significant changes for pore size less than 10 nm. These variations are due to the difference in the increased rate of the oil and gas pressures (capillary pressure). Jin et al. used three different mixtures as per composition. Two-phase envelopes were developed for a mixture of (1) C_1 (30 mol%)-nC_4 (35 mol%)-C_8 (35 mol%) and for (2) C_1(10 mol%)-nC_4 (25 mol%)-C_8 (65 mol%). The two phase envelopes for these two mixtures did not exhibit any significant difference as the pore size was reduced from infinite to 100 nm (Figure 2.7). This observation was in agreement with the experimental results of Sigmund et al. (1973).

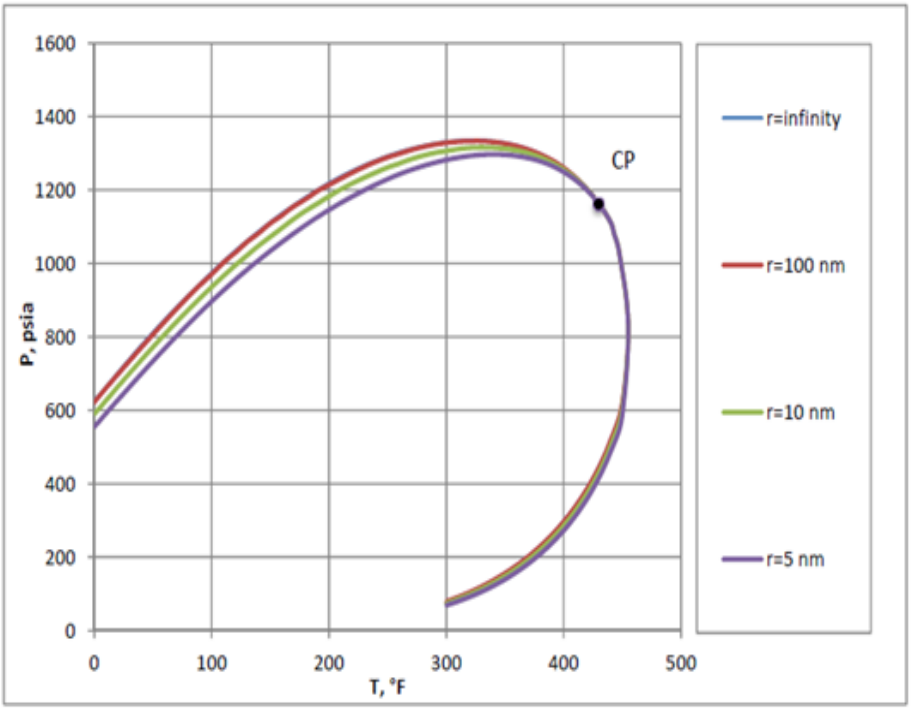

Figure 2.7: Phase envelopes for C_1 (30 mol%)-nC_4 (35 mol%)-C_8 (35 mol%) mixtures at different pore radius (Method 1) (Jin et al., 2013)

Two-phase envelope is significantly reduced by decreasing the pore size less than 10 nm (Figure 2.8). With the decrease of pore size, the bubble point pressures decrease and the lower dew point pressures increase at all temperatures. The change in bubble point is because of the fact that adsorption becomes significant in pore radius less than 10 nm (Shapiro and Stenly, 1996; Udell, 1982).

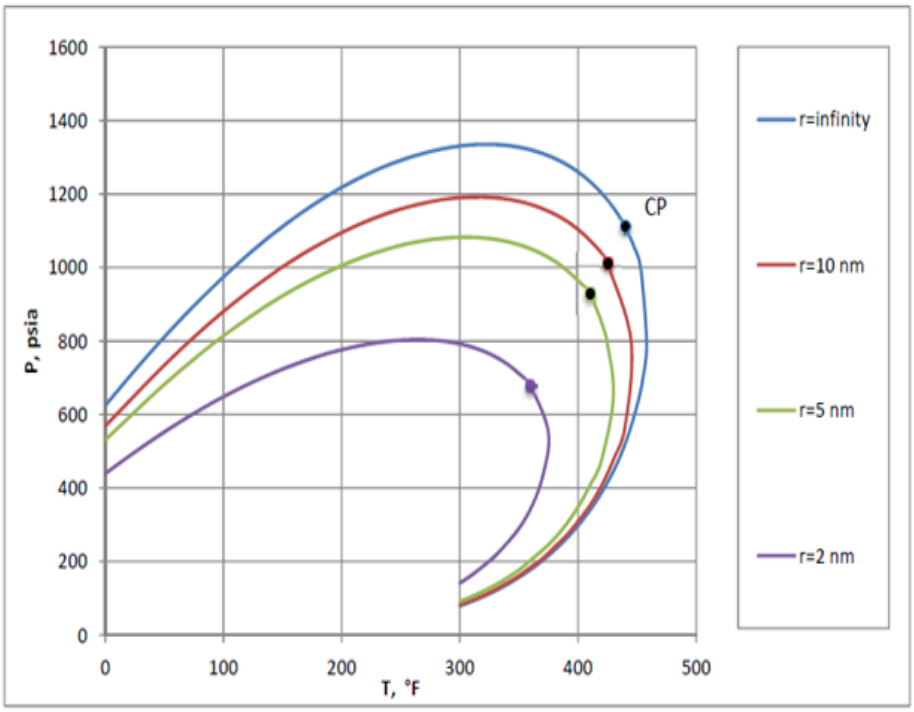

Figure 2.8: Phase envelopes for C_1 (30 mol%)-nC_4 (35 mol%)-C_8 (35 mol%) mixtures at different pore radius (Method 2) (Jin et al., 2013)

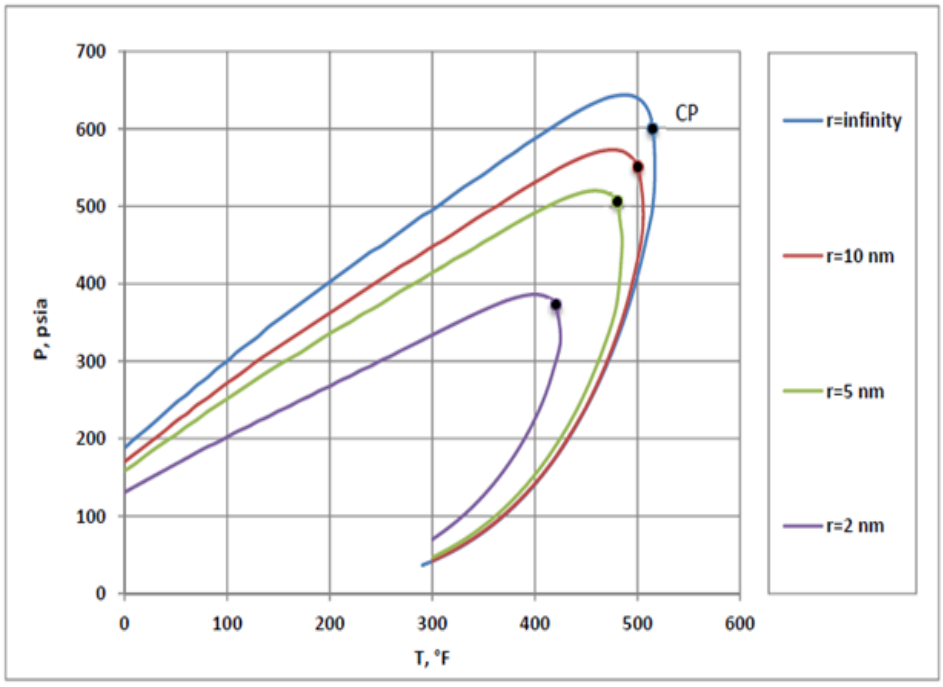

Figure 2.9: Phase envelopes for C_1 (10 mol%)-nC_4 (25 mol%)-C_8 (65 mol%) mixtures at different pore radius (Method 2) (Jin et al., 2013)

According to Jin et al. (2013), interfacial tension for bulk fluid and confined fluid remain approximately the same for pore sizes more than 50 nm as well as for less than 50 nm pore size with their first method. However, the interfacial tension decreases dramatically for pore size less than 10 nm when second method was implemented. The critical point does not change when method 1 is implemented. The closer the temperature is to the critical point, the smaller will be the change in saturation pressure. The critical point decreases with reduction in pore size when method 2 is implemented (Figure 2.9).

Capillary pressure also plays a significant role in phase behavior in tight rocks and shales. According to Kuila and Prasad (2011), the matrix in shale reservoirs consists of micropores smaller than 2 nm in diameter to mesopores with diameters of range 2 to 50 nm. If increased capillary pressure is not accounted in small pores like that of shales, it could lead to inaccurate estimates of saturation pressures and ultimate recovery. Large capillary pressure also decreases the in-situ oil density, which affects the oil formation volume factor and ultimate reserves calculations. Study performed by B.Nojabaei et al. (2013) shows that the change in saturation pressures, fluid densities, and viscosities is highly dependent on the capillary pressure used in the calculations. Firincioglu et al. (2012) performed flash calculation using Peng-Robinson equation of state (1976 EOS) considering both surface and capillary forces. Their result show that surface forces are small compared with capillary forces for pores larger than approximately 1 nm. Ping et al. (1996) developed a theoretical model for calculating the dew-point by considering the effect of capillary pressure and adsorption in porous media. This showed that capillary pressure and adsorption increased the dew-point pressure.

B.Nojabaei et al. (2013) determined the phase envelopes for variety of binary mixtures with interaction parameters for all mixtures set to 0.005. The hydrocarbon components taken were C_1, C_3, C_4, C_6 and C_{10} with Parachor coefficients of 77.33, 151.90, 191.70, 271.0 and 392.25 respectively. The phase envelopes were developed for the binary mixtures as C_1/C_3, C_1/C_4, C_1/C_6 and

C_1/C_{10} at a fixed pore radius of 10 nm and a fixed mole fraction of 70% for C_1. The phase envelope in Fig. 2.10 shows that the effect of capillary pressure reduces the bubble-point pressure across all temperatures, but the bubble-point suppression decreases to zero at critical point.

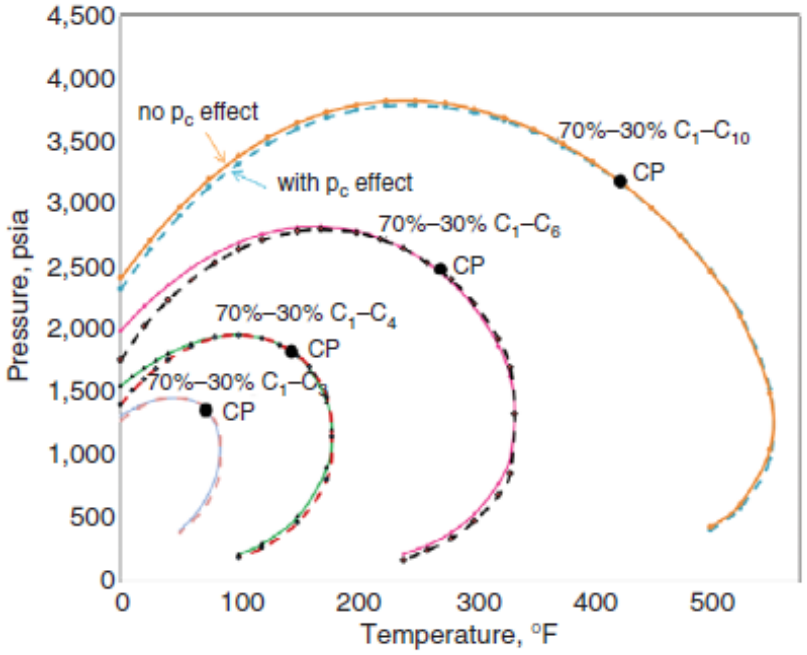

Figure 2.10: Phase envelopes with and without capillary pressure for binary mixtures (70:30 C_1/C_4 and 70:30 C_1/C_6) and pore radius of 10 nm. (B.Nojabaei et al., 2013)

Phase envelopes for different C_1/C_6 mixtures at fixed pore radius of 20 nm were plotted by B.Nojabaei et al. (2013) during their study. It has been observed that effect of capillary pressure is more prominent in heavier mixtures when compared at the same temperature. This behavior is more pronounced at a fixed temperature because the heavier mixture compositions are generally further

from the critical point and their respective bubble-point pressures are lower. When the critical temperature and cricondentherm approach each other, the fluids become heavier. This results in decrease of the size of the region where dew-point pressures are increased by capillary pressure. It was also found that capillary pressure changes the fluid densities and in general, this effect becomes more prominent for gas density as the pressure and temperature point moves within the two-phase region and away from the dew-point pressure curve

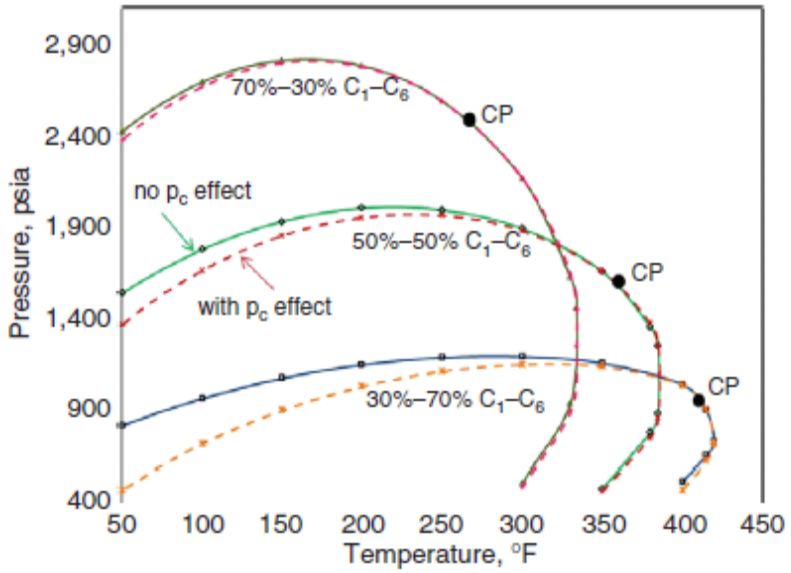

Figure 2.11: Phase envelopes for various C_1/C_6 mixtures and pore radius of 20 nm. (B.Nojabaei et al., 2013)

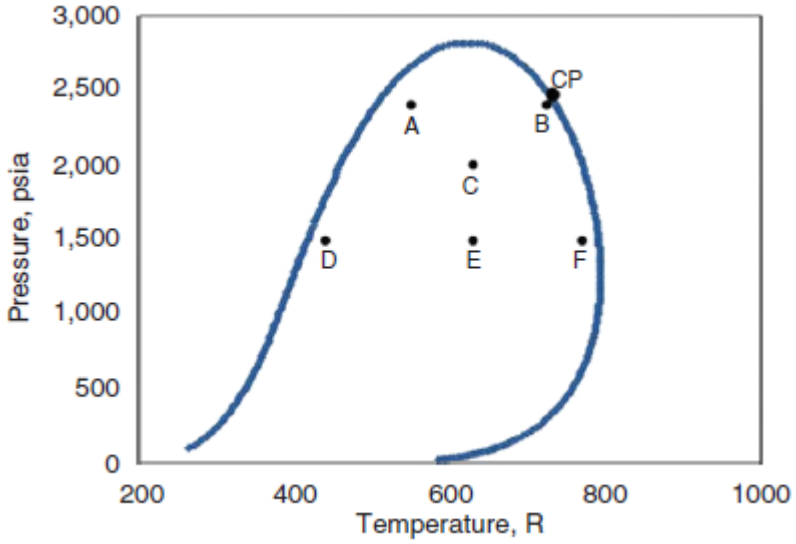

Figure 2.12: Temperature and pressure points within the two-phase region for the 70:30 C_1/C_6 mixtures. (B.Nojabaei et al., 2013)

CHAPTER 3: RESEARCH APPROACH

Given that the main objective of this work is to study the feasibility of a new experimental approach in studying phase behavior under confinement, the research approach was concerned with simulating some of the experimental procedures so that we can determine whether these results can be used to experimentally detect the edge of the phase envelope. In this chapter, we present the details of this research approach.

3.1 SIMULATION INPUT/FEED

We used a commercial simulator to collect that data needed, however, since the experiment we were designing is not a conventional experiment, we had to use the simulator to generate row data and then use this data to be able to develop experimental predictions.

3.1.1 SOFTWARE: CMG-WinProp®

WinProp is CMG's equation of state (EOS) multiphase equilibrium and properties determination program. WinProp features techniques for characterizing the heavy ends of the petroleum fluids, lumping of components, matching laboratory PVT data through regression, simulation of first and multiple contact miscibility, phase diagrams construction and more. Laboratory experiments considered in WinProp include recombination of separator oil and gas, compressibility measurements along with the PVT experiments such as

differential liberation, constant volume depletion, and constant composition expansion.

WinProp can be used to predict phase behavior of reservoir fluids as well as characterize these fluids for reservoir simulation. It requires some knowledge of phase behavior as it pertains to the different fluid types found in reservoirs. It allows user to prepare data, view plots of the input, run the phase property calculation engine and subsequently, view the text file and graphical results.

3.1.2 EQUATION OF STATE USED FOR SIMULATION

WinProp has options to select from various equations of state for the oil and gas phases. The equations are: Equation of State

PR(1978)	Peng-Robinson equation of state with 1978 expression for constant "a".
PR(1976)	Peng-Robinson equation of state with 1976 expression for constant "a". This is the original equation of state.
SRK(G&D)	Soave-Redlich-Kwong equation of state with the constant "a" proposed by Grabowski and Daubert.
SRK	Original Soave-Redlich-Kwong equation of state.

The default equation of state is Peng-Robinson EOS (1978). In this work, we compared the results from PR(1978) and SRK(G&D) and the results were identical (presented in the following chapter).

3.1.3 DEFINING COMPOSITION

For determining various properties of fluids, equation of state requires some properties of each component (which are present in the fluid) along with the mole fractions or mole percent and mass fractions or mass percent. The most basic properties required for the prediction of equation of state for each component are critical temperature (T_C), critical pressure (P_C), acentric factor (ω) and interaction coefficients between different components.

Defining or selection of components can be done in two ways. There are several components such as pure hydrocarbons, petroleum fractions, light gases etc. that are already listed in the Library Components and these can be directly selected. The selection of components from the library automatically lists their respective properties. Another way to define components is by custom editing or editing the component properties either by specifying critical properties, or by specifying physical properties and calculating critical properties using various correlations. For example, the user may input the component name followed by the critical temperature, critical pressure, acentric factor and molecular weight if the direct critical property specification is the desired method. Desired Physical Properties Correlation and Critical Properties Correlation can be selected as necessary.

3.1.4 COMPOSITION SPECIFICATION (WINPROP® HELP)

Compositions are entered in moles or in weight units, specified as fraction or percent. Values are always being normalized internally when the simulation is run. Clicking the normalize button lets the user normalize the values in the composition table. If weight fractions or weight percentages are entered, they are converted internally to mole fractions. Generally, the primary composition corresponds to the composition of the oil or gas in place. Values must be entered for the primary composition. The secondary composition corresponds normally to the injected fluid. The secondary composition need not be entered and will default to zero.

The feed composition used for all calculation options can be:

- a mixture of the primary composition and the secondary composition
- the feed from the previous calculation option
- the vapor composition from the previous calculation option
- the liquid composition from the previous calculation option
- the composition of any phase from the previous calculation option

3.1.5 OUTPUT DATA GENERATED

Flash calculations were carried out to determine the split of a system at a given temperature, pressure and feed composition. The determination of number of phases and the properties for each phases were also calculated using flash calculations. Winprop can perform many different types of flash calculations:

1. Two-phase vapor-liquid
2. Three-phase vapor-liquid$_1$-liquid$_2$
3. Three-phase vapor-liquid-aqueous
4. Four phase flash calculation (fluid phases only)
5. Multiphase flash calculations with a solid phase
6. Isenthalpic flash calculation

Two-phase vapor-liquid and Multiphase flash calculation were carried out for the requirement of the simulations conducted in this study. The output generated for both liquid and vapor phase include:

- Z-factor
- Molar volume
- Molecular Weight
- Ideal Heat
- Enthalpy
- Entropy
- Density
- Viscosity
- IFT
- Phase volume percent
- Phase mole percent

Moreover, the two-phase diagram construction was achieved by manually entering the input parameters such as initial conditions of pressure and

temperature, variable limits i.e. minimum and maximum pressure and temperature, compressibility factor of liquid and vapor phase. Number of iterations and specification variable number were automatically calculated.

3.2 – SIMULATION APPROACH AND CALCULATION

Given that one experimental limitation we have in this new approach is that the volume as well as the overall composition had to be fixed throughout the experiment, our only variables were pressure and temperature. The idea is to start at a given temperature and pressure point outside the phase envelope, lower the temperature and calculate the corresponding pressure. The goal is to see whether were the bulk phase behavior, the plot of pressure as a function of temperature for a given system can be used to detect the phase envelope.

3.2.1 APPROACH IMPLEMENTED

Phase behavior simulation and Flash calculation for various two component hydrocarbon systems were carried out, followed by generation and comparison of results. The basic molar composition for all the system was 50% - 50% of each hydrocarbon. The systems studied were:

1. Ethane – Butane
2. Ethane – Pentane
3. Ethane – Hexane, and
4. Ethane – Heptane.

Two-phase envelope was also generated by simulation for the above systems. All the data points and coordinates were later used for development of phase diagram and to determine the Pressure-temperature relation for a given set of hydrocarbons. All the simulation results for two-phase envelop and multiphase flash calculations are shown in next chapter.

The study after that focused on Ethane – Pentane for experimental feasibility, and this system with different composition and initial temperature and pressure was further studied. The different compositions studied were:

1. 50% Ethane – 50% Pentane
2. 40% Ethane – 60% Pentane
3. 40% Ethane – 60% Pentane with initial pressure of 800 psi, and
4. 40% Ethane – 60% Pentane with initial pressure of 600 psi.

3.2.2 CALCULATION

For each fluid system that was studied, a bulk phase envelope was generated, and then a matrix of pressure and temperature values was generated to determine the fluid properties at each temperature and pressure value in this matrix. The properties we needed to obtain from flash calculations to use in our calculations were the vapor phase z-factor, vapor phase volume percent and vapor phase mole percent values. It was needed to be able to calculate the pressure in the system as temperature is reduced.

Values for vapor phase z-factor, vapor phase volume percent and vapor phase mole percent at each temperature and pressure was entered in the matrix. The choice of pressure and temperature values for the matrix were based on the phase envelope and critical point of the system. Near the edge of the phase envelope, small intervals were used in pressure and temperature to increase the accuracy and be able to detect phase change. An example of such matrices can be seen in table No. 4.4, 4.5, and 4.6.

3.2.3 EXCEL FILE BUILD UP

Various calculations were carried out to get the pressure values at the experimental temperatures.. The total volume 'V' of the system was kept constant at 25 cubic centimeter or 0.000883 cubic feet. Initial pressure and initial temperature was a reference condition in the phase diagram at which the system was in single gaseous phase. Real gas equation was used to get the total number of moles 'n' for the system according to the conditions using the following equation,

$$PV = ZnRT$$

So,

$$n = \frac{PV}{zRT}$$

The number of moles in vapor phase 'n_g' and volume in vapor phase 'v_g' at each value of pressure and temperature in the matrix were calculated using the values of vapor phase mole percent and vapor phase volume percent.

In order to use this data to predict the experimental pressure value as temperature as reduced, we made use of the following equation,

$$\frac{Pv_g}{zn_g} = RT$$

A matrix was generated to calculate "P* v_g / z* n_g" for each value of pressure and temperature using the matrices that were generated for 'n_g' and 'v_g'. For each temperature, the goal was then to determine the "P* v_g / z* n_g" value that corresponds to the value of 'R*T' at that temperature. To achieve this, a "P* v_g / z* n_g" Versus "P" plot was made for each temperature (example can be seen in Fig 4.7). On each temperature line within the plot, the 'Pressure' was determined referring to 'R*T' values as: P* v_g / z* n_g = R*T.

A plot was the developed with these pressure values and the corresponding temperature values. This plot of Pressure vs. Temperature shows the point of phase change i.e. from single phase to two phase, of a given system, which can be identified through the change in the slope of the line. This is confirmed when superimposed over the phase diagram. The temperature at which the P vs. T line crosses the two-phase envelope denotes the point of phase change in that system and coincides with the change in slope of the line.

CHAPTER 4: RESULTS

In this chapter, we present the results of the simulation for the various binary systems that were considered in this study and we then zoom-in on the system that we considered to be the best choice for conducting experiments.

4.1 – PHASE BEHAVIOR SIMULATIONS FOR VARIOUS TWO-COMPONENT HYDROCARBON SYSTEMS

For each of the binary systems considered, we here present the result of the simulation of the experimental process. The result is simply a plot of the expected pressure value at each temperature step as temperature is lowered under constant volume/constant composition conditions.

1. 50% Ethane – 50% Butane

For this system, the bulk phase diagram is shown in Fig. 4.1. An ideal starting point for this system in terms of temperature and pressure would be at 300 F and 900 psi since this is a point at which the whole mixture is in the gas phase and it's far enough from the phase envelope to give enough data points outside the envelope and be able to detect the edge. The matrices of data from the simulation runs for this system are presented in Appendix A. Following the process described in section 3.2.3, the pressure value corresponding to various temperature steps were calculated, shown in Table 4.1. A plot of these values projected on the phase diagram is shown in Fig. 4.2.

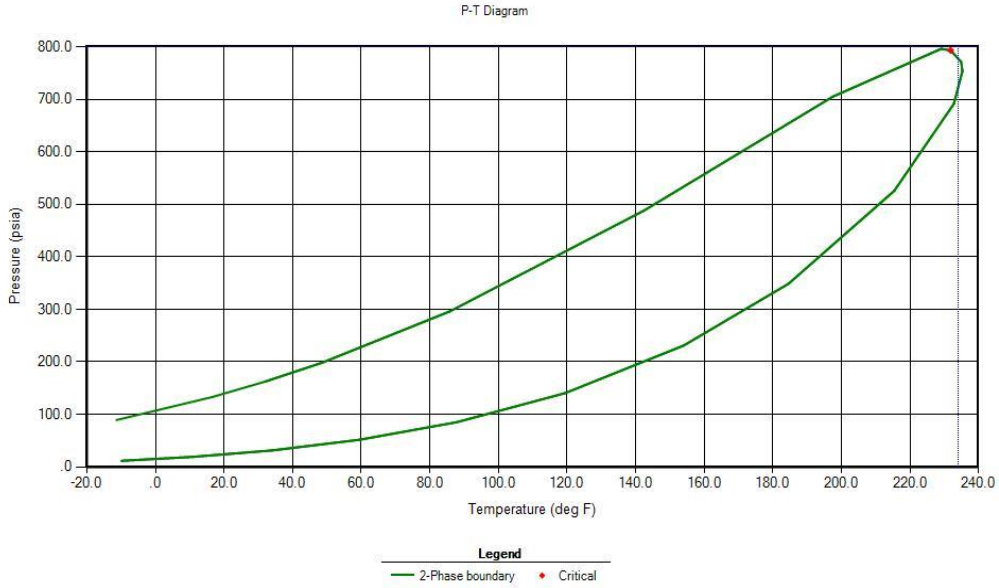

Figure 4.1: Two phase diagram of 50% Ethane – 50% Butane

Table 4.1: Pressure at each Temperature step for 50% Ethane – 50% Butane

T (in F)	P (in psi)
300	900
260	772
245	722
230	672
215	615
200	560
185	505
170	460
140	368

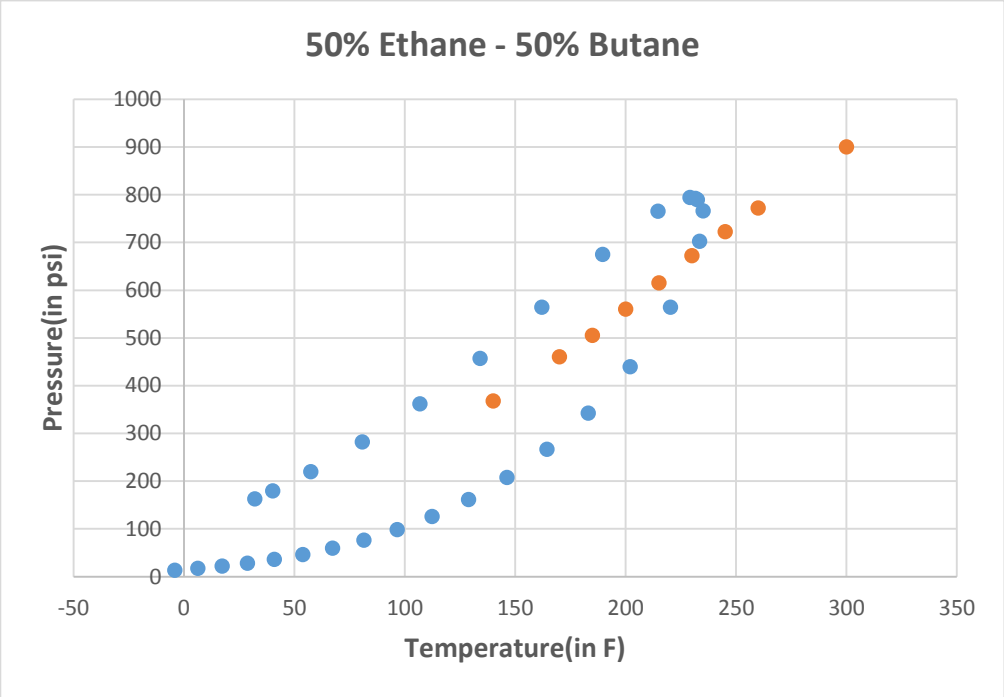

Figure 4.2: Two phase diagram of 50% Ethane – 50% Butane with superimposed Pressure versus Temperature plot

The results for this system show that there is not a significant change in slope at the border of the phase envelope, suggesting that this is not a good system for experimental testing of this new process. There is a small change in slope, but not large enough that it can be detected with experimental measurements.

2. 50% Ethane – 50% Hexane

We now consider the ethane/hexane system at 50 mole perfect each. The phase diagram for this system is shown in Fig. 4.3. A suitable starting point for this system we chosen to be at 400 F and 1000 psi. The tabulated data of pressure

calculate for various temperature values is shown in Table 4.2. The row data used to generate these pressure values are presented in Appendix B. The overlap of the pressure data with the phase envelope are shown in Fig. 4.4.

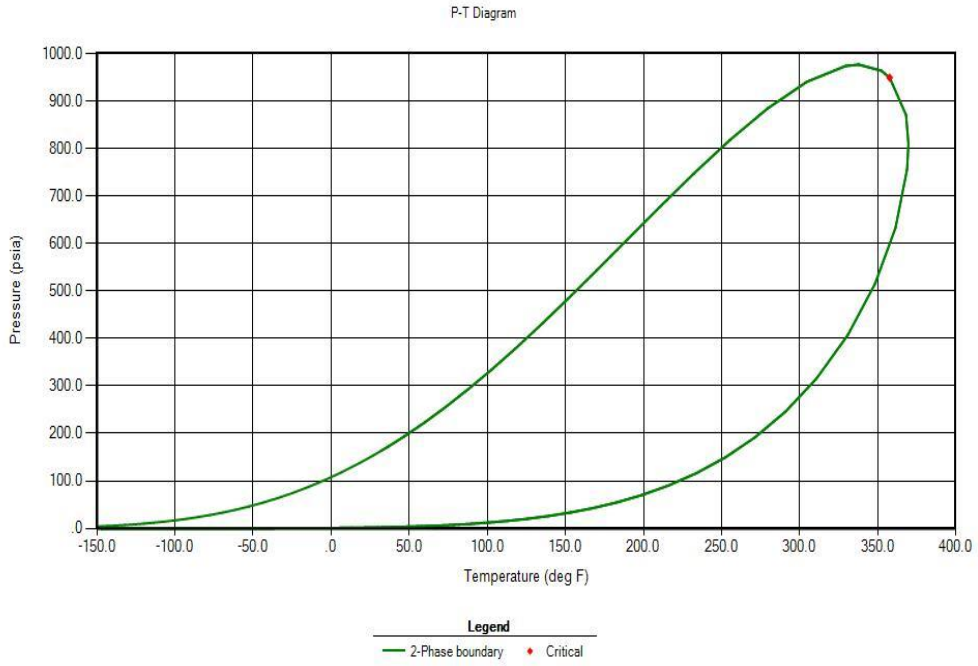

Figure 4.3: Two phase diagram of 50% Ethane – 50% Hexane

Table 4.2: Pressure at each Temperature step for 50% Ethane – 50% Hexane

T (in F)	P (in psi)
400	1000
380	923
370	884
360	845
350	812
345	795
340	782
330	750
325	735
310	698
280	615
250	548
220	480

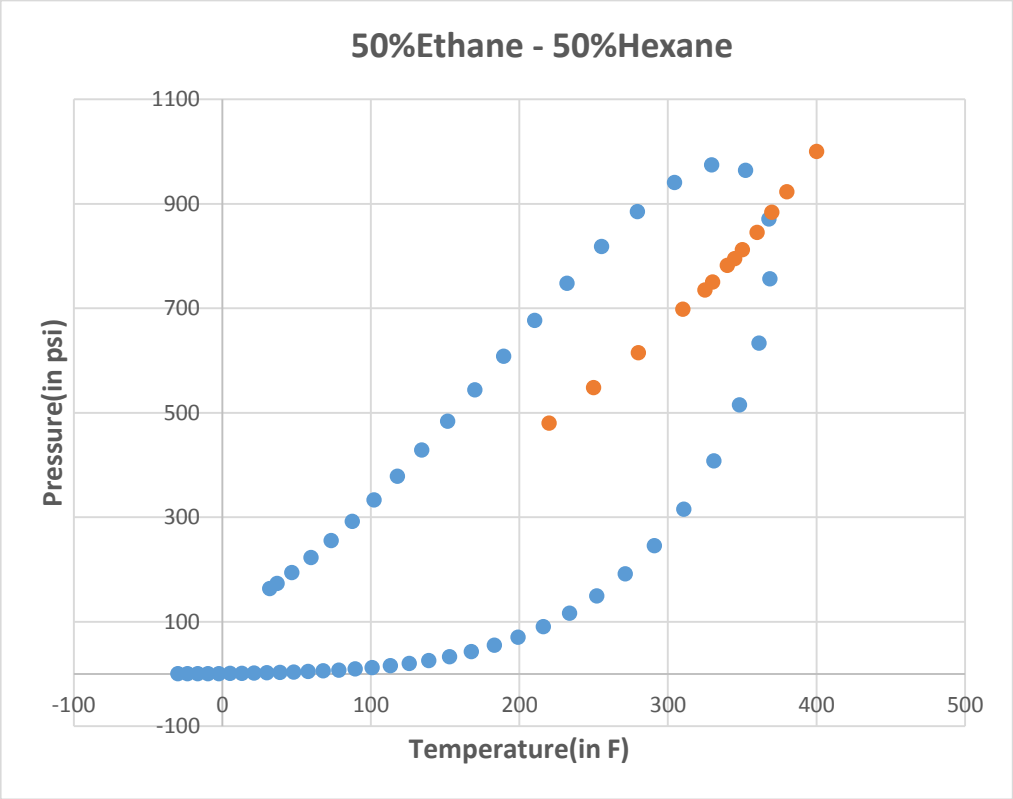

Figure 4.4: Two phase diagram of 50% Ethane – 50% Hexane with superimposed Pressure versus Temperature plot

The result for this system suggests that there is a significant change in slope as the system enters the two-phase region, however the temperature requirement for the starting point of 400 F is higher than our experimental capabilities and it was decided to pursue other systems, but this was an evidence that it is possible for some systems to detect the edge of the phase envelope by simply changing temperature and reading pressure.

3. 50% Ethane – 50% Heptane

The results for this system are shown in Fig 4.5, Table 4.3 and Figure 4.6.

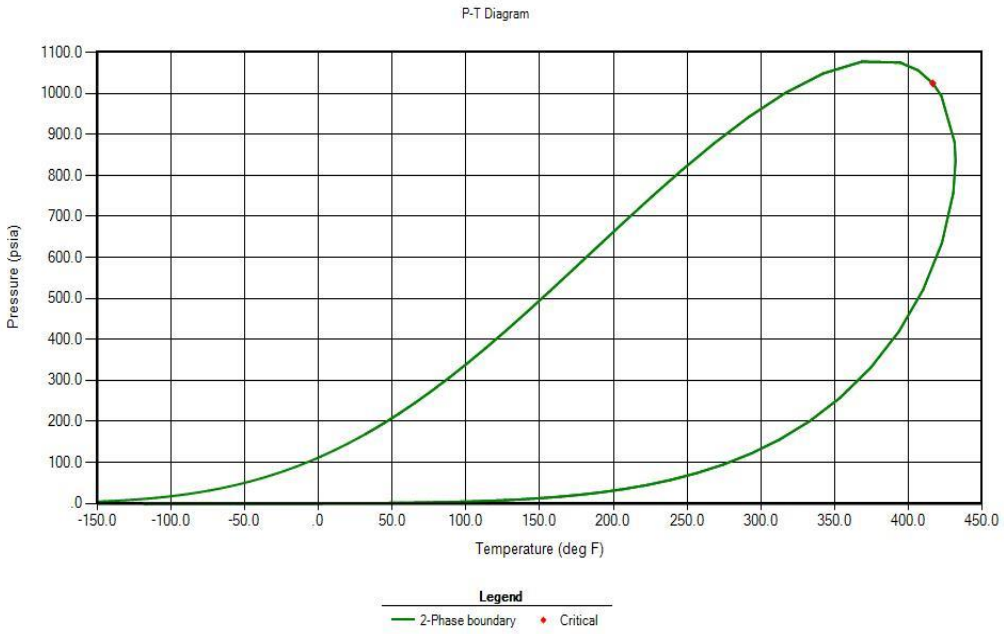

Figure 4.5: Two phase diagram of 50% Ethane – 50% Heptane

Table 4.3: Pressure at each Temperature step for 50% Ethane – 50% Heptane

T (in F)	P (in psi)
530	1198
510	1135
490	1070
460	972
430	873
420	845
400	789
360	689

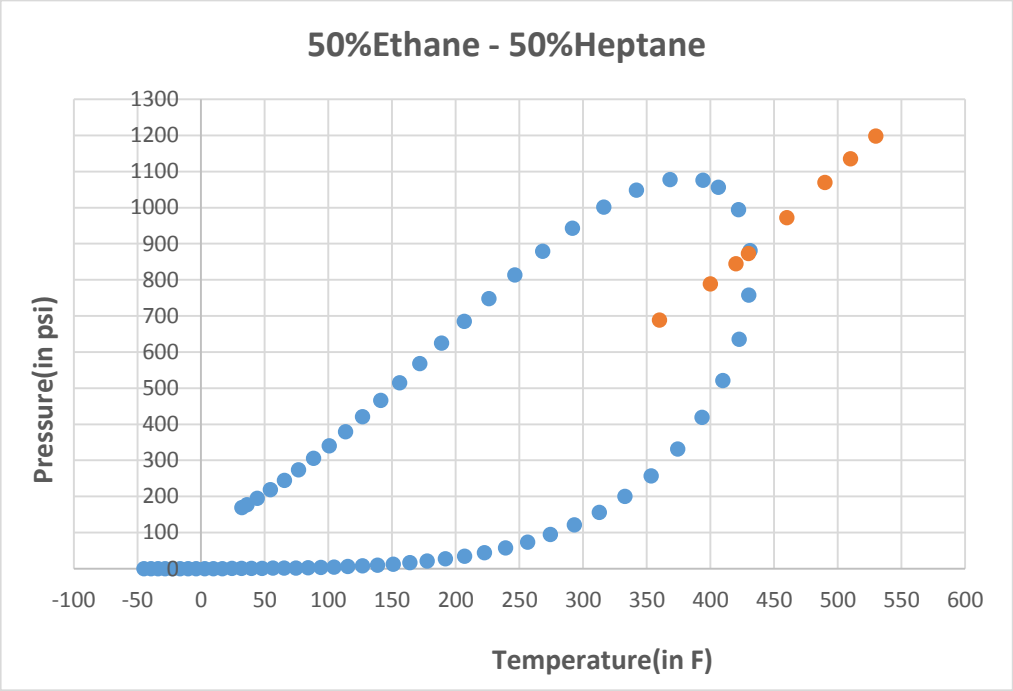

Figure 4.6: Two phase diagram of 50% Ethane – 50% Heptane with superimposed Pressure versus Temperature plot

The result for this system, as for the previous one, shows that there is enough change in slope to have experimental detection, but the temperature requirements are too high. The details of the calculations for this system are presented in Appendix C.

4.2 THE ETHANE-PENTANE SYSTEM

After running the phase behavior analysis of various components, it was decided to zoom-in on this system due to the following reasons:

- The choice of initial temperature and pressure seems to be a practical choice for this system as it is within the experimental constraints. Some

other systems require temperatures that the current lab equipment cannot handle.

- The break in slope as this systems transitions from single to two phase is very clear. This makes it easier to experimentally detect this transition even with the presence of experimental errors and limitations.

1. 50%Ethane – 50%Pentane

The phase diagram for this system is shown in Fig. 4.7. A suitable initial point based on this phase diagram is 350 F and 1000 psi. We now present the data that were collected for this system to determine the pressure value for each temperature starting from the initial point. In tables 4.4, 4.5 and 4.6 below we present the matrices of the z-factor for vapor phase, the volume percent of gas and the mole percent of gas at various temperature and pressure values. In tables 4.7 and 4.8 we show the calculated number of moles and volume for the gas phase that are used in the calculations. Following that, in table 4.9, the value of PV/nZ is presented in matrix form as well. Data from table 4.9 is presented graphically in Fig. 4.8 as a function of pressure for various temperature values. This figure is the one used to generate the pressure-temperature data expected from the experiments.

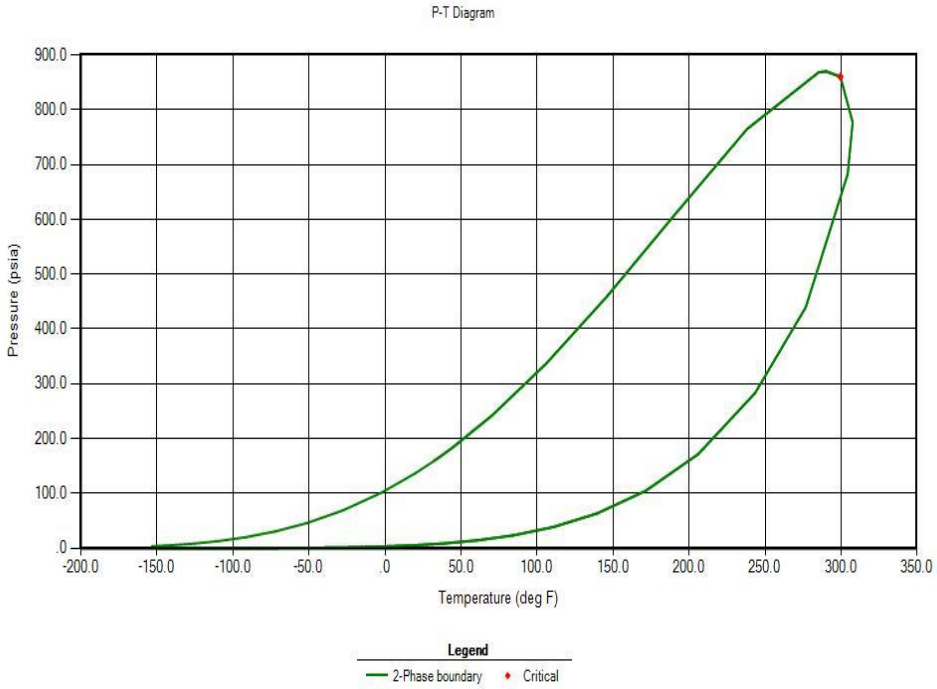

Figure 4.7: Two phase diagram of 50% Ethane – 50% Pentane

Table 4.4: Z-factor of 50% Ethane – 50% Pentane system

Z-factor for Gas									
Pressure	**1000**	**900**	**860**	**830**	**800**	**700**	**600**	**500**	**400**
Temperature									
350	0.5297	0.5657	0.5829	0.5965	0.6107	0.6604	0.7115	0.7623	0.8122
340	0.4993	0.5359	0.5543	0.5691	0.5845	0.6390	0.6947	0.7496	0.8029
330	0.4669	0.5024	0.5217	0.5377	0.5547	0.6150	0.6763	0.7358	0.7929
320	0.4335	0.4649	0.4844	0.5015	0.5200	0.5876	0.6558	0.7208	0.7821
310	0.4011	0.4241	0.4420	0.4591	0.4790	0.5556	0.6327	0.7043	0.7705
300	0.3718	0.3832	0.3961	0.4547	0.4847	0.5493	0.6062	0.686	0.7579
290	0.3470	0.3470	0.4544	0.4856	0.5092	0.5679	0.6128	0.6656	0.7442
280	0.3267	0.3183	0.4822	0.5072	0.5280	0.5835	0.6278	0.6654	0.7293
260	0.2974	0.2803	0.274	0.2696	0.5542	0.6071	0.6514	0.6903	0.7246
230	0	0	0	0	0	0.6264	0.6731	0.7152	0.7534
200	0	0	0	0	0	0	0.6799	0.7265	0.7695

Table 4.5: Vapor phase volume percent of 50% Ethane – 50% Pentane system

Vapor Phase Volume %									
Pressure	**1000**	**900**	**860**	**830**	**800**	**700**	**600**	**500**	**400**
Temperature									
350	100	100	100	100	100	100	100	100	100
340	100	100	100	100	100	100	100	100	100
330	100	100	100	100	100	100	100	100	100
320	100	100	100	100	100	100	100	100	100
310	100	100	100	100	100	100	100	100	100
300	100	100	100	74.1513	81.0972	94.3439	100	100	100
290	100	100	21.6921	49.3726	63.0046	85.0307	95.4559	100	100
280	100	100	4.9462	32.2424	48.5881	76.7243	90.0762	97.7883	100
260	100	100	100	100	18.8878	60.3226	79.9104	90.8893	97.6505
230	0	0	0	0	0	25.7082	62.3105	80.5533	90.8723
200	0	0	0	0	0	0	29.3	66.5043	83.598

Table 4.6: Vapor phase mol percent of 50% Ethane – 50% Pentane system

Vapor Phase Mol %									
Pressure	**1000**	**900**	**860**	**830**	**800**	**700**	**600**	**500**	**400**
Temperature									
350	100	100	100	100	100	100	100	100	100
340	100	100	100	100	100	100	100	100	100
330	100	100	100	100	100	100	100	100	100
320	100	100	100	100	100	100	100	100	100
310	100	100	100	100	100	100	100	100	100
300	100	100	100	67.6601	72.8775	88.0997	100	100	100
290	100	100	17.044	38.2361	48.9747	70.1341	86.9437	100	100
280	100	100	3.2837	21.5409	32.949	56.2117	73.2168	91.152	100
260	100	100	100	100	9.7267	35.0203	52.427	68.2684	87.2046
230	0	0	0	0	0	10.0408	29.5374	45.079	60.0639
200	0	0	0	0	0	0	9.0457	27.1116	42.1336

Table 4.7: Number of mole in vapor phase of 50% Ethane – 50% Pentane system

n_g									
Pressure	**1000**	**900**	**860**	**830**	**800**	**700**	**600**	**500**	**400**
Temperature									
350	0.000192	0.000192	0.000192	0.000192	0.000192	0.000192	0.0001918	0.000192	0.000192
340	0.000192	0.000192	0.000192	0.000192	0.000192	0.000192	0.0001918	0.000192	0.000192
330	0.000192	0.000192	0.000192	0.000192	0.000192	0.000192	0.0001918	0.000192	0.000192
320	0.000192	0.000192	0.000192	0.000192	0.000192	0.000192	0.0001918	0.000192	0.000192
310	0.000192	0.000192	0.000192	0.000192	0.000192	0.000192	0.0001918	0.000192	0.000192
300	0.000192	0.000192	0.000192	0.00013	0.00014	0.000169	0.0001918	0.000192	0.000192
290	0.000192	0.000192	3.27E-05	7.33E-05	9.39E-05	0.000135	0.00016676	0.000192	0.000192
280	0.000192	0.000192	6.3E-06	4.13E-05	6.32E-05	0.000108	0.00014043	0.000175	0.000192
260	0.000192	0.000192	0.000192	0.000192	1.87E-05	6.72E-05	0.00010055	0.000131	0.000167
230	0	0	0	0	0	1.93E-05	5.6652E-05	8.65E-05	0.000115
200	0	0	0	0	0	0	1.7349E-05	5.2E-05	8.08E-05

Table 4.8: Vapor phase volume of 50% Ethane – 50% Pentane system

V_g									
Pressure	**1000**	**900**	**860**	**830**	**800**	**700**	**600**	**500**	**400**
Temperature									
350	0.000883	0.000883	0.000883	0.000883	0.000883	0.000883	0.000883	0.000883	0.000883
340	0.000883	0.000883	0.000883	0.000883	0.000883	0.000883	0.000883	0.000883	0.000883
330	0.000883	0.000883	0.000883	0.000883	0.000883	0.000883	0.000883	0.000883	0.000883
320	0.000883	0.000883	0.000883	0.000883	0.000883	0.000883	0.000883	0.000883	0.000883
310	0.000883	0.000883	0.000883	0.000883	0.000883	0.000883	0.000883	0.000883	0.000883
300	0.000883	0.000883	0.000883	0.000655	0.000716	0.000833	0.000883	0.000883	0.000883
290	0.000883	0.000883	0.000191	0.000436	0.000556	0.000751	0.000843	0.000883	0.000883
280	0.000883	0.000883	4.37E-05	0.000285	0.000429	0.000677	0.000795	0.000863	0.000883
260	0.000883	0.000883	0.000883	0.000883	0.000167	0.000533	0.000705	0.000802	0.000862
230	0	0	0	0	0	0.000227	0.00055	0.000711	0.000802
200	0	0	0	0	0	0	0.000259	0.000587	0.000738

Table 4.9: $P*v_g/Z*n_g$ chart of 50% Ethane – 50% Pentane system

$P*V_g/Z*n_g$									
Pressure	**1000**	**900**	**860**	**830**	**800**	**700**	**600**	**500**	**400**
Temperature									
350	8689.378	7322.764	6790.833	6404.516	6029.492	4878.762	3881.459	3018.998	2266.813
340	9218.433	7729.963	7141.217	6712.869	6299.762	5042.151	3975.325	3070.147	2293.07
330	9858.136	8245.397	7587.458	7104.88	6638.203	5238.918	4083.481	3127.727	2321.99
320	10617.68	8910.491	8171.711	7617.735	7081.175	5483.211	4211.129	3192.816	2354.054
310	11475.35	9767.714	8955.604	8321.268	7687.288	5799.018	4364.878	3267.616	2389.494
300	12379.68	10810.25	9993.378	9207.844	8453.724	6281.256	4555.688	3354.784	2429.22
290	13264.45	11938.00	11086.87	10158.52	9302.951	6878.463	4947.842	3457.605	2473.939
280	14088.66	13014.41	12365.11	11274.08	10284.01	7536.715	5411.877	3710.45	2524.483
260	15476.68	14778.76	14446.63	14170.23	12902.03	9141.484	6462.052	4438.578	2845.217
230	-	-	-	-	-	13169.47	8655.244	5750.032	3697.184
200	-	-	-	-	-	-	13156.8	7770.476	4747.198

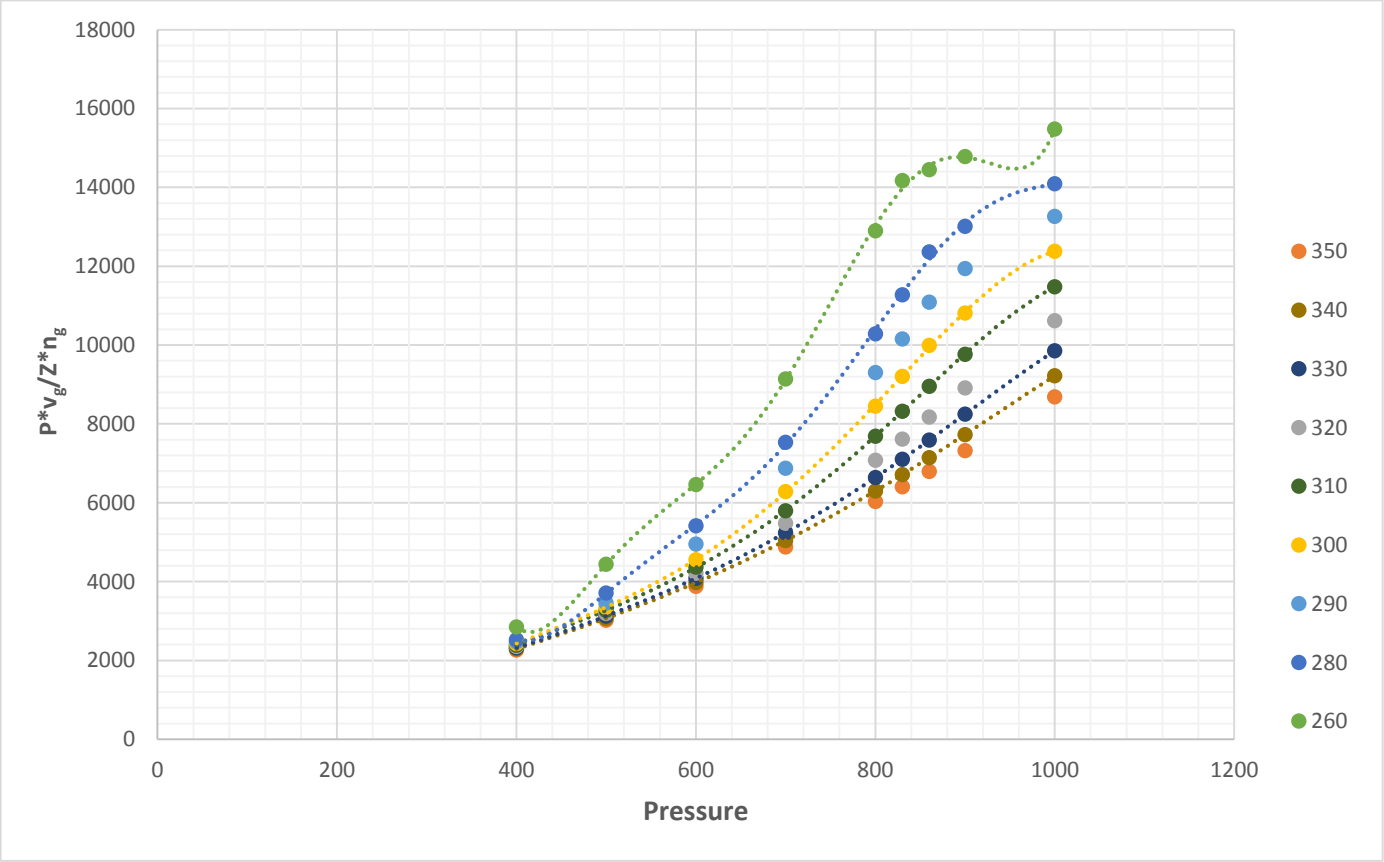

Figure 4.8: P^*v_g/Z^*n_g versus Pressure of 50% Ethane – 50% Pentane

Table 4.10 below shows the pressure values corresponding to the various temperature steps for this system as obtained from Fig. 4.8. A plot of these data is shown in Fig.4.9. These results seem promising as it shows a slope change in the data. Overlapping that data on the phase diagram is shown in Fig.4.10 indicates that the slope change does correspond to the edge of the phase envelope. Because the results with the 50/50 system showed promise and results within experimental capabilities, we decided to explore other ethane-pentane mixtures.

Table 4.10: Pressure at each Temperature step for 50% Ethane – 50% Pentane

T (in F)	P (in psi)
350	1000
340	958
330	914
320	874
310	828
300	784
290	746
280	718
260	656

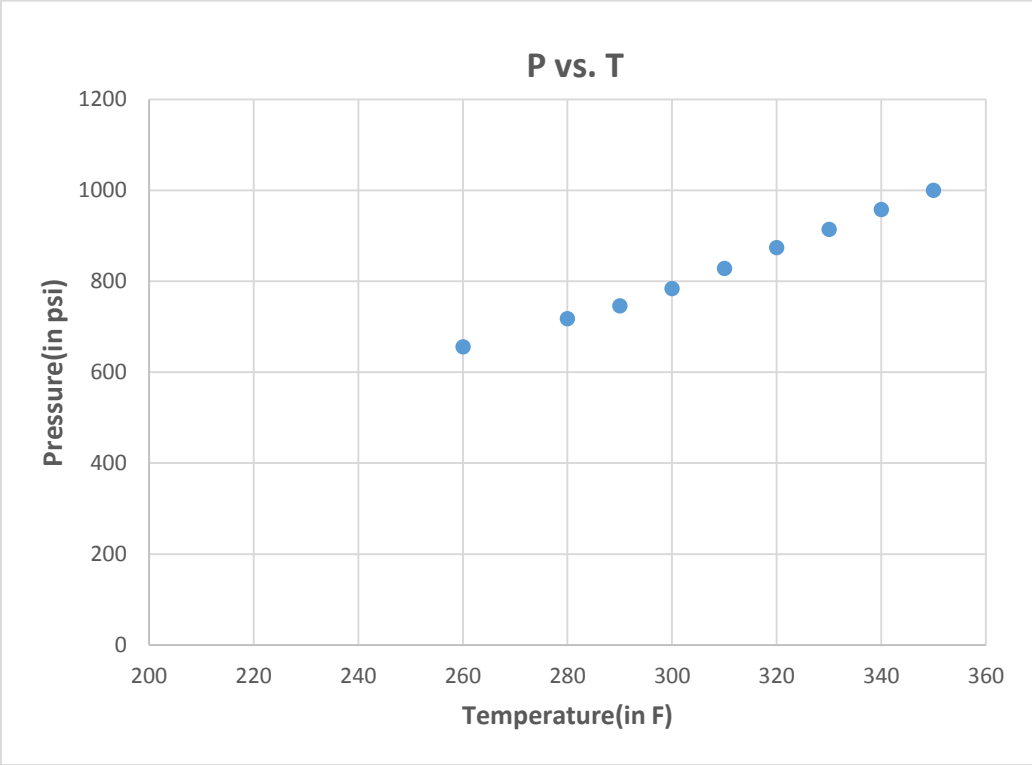

Figure 4.9: Pressure versus Temperature of 50%Ethane – 50%Pentane

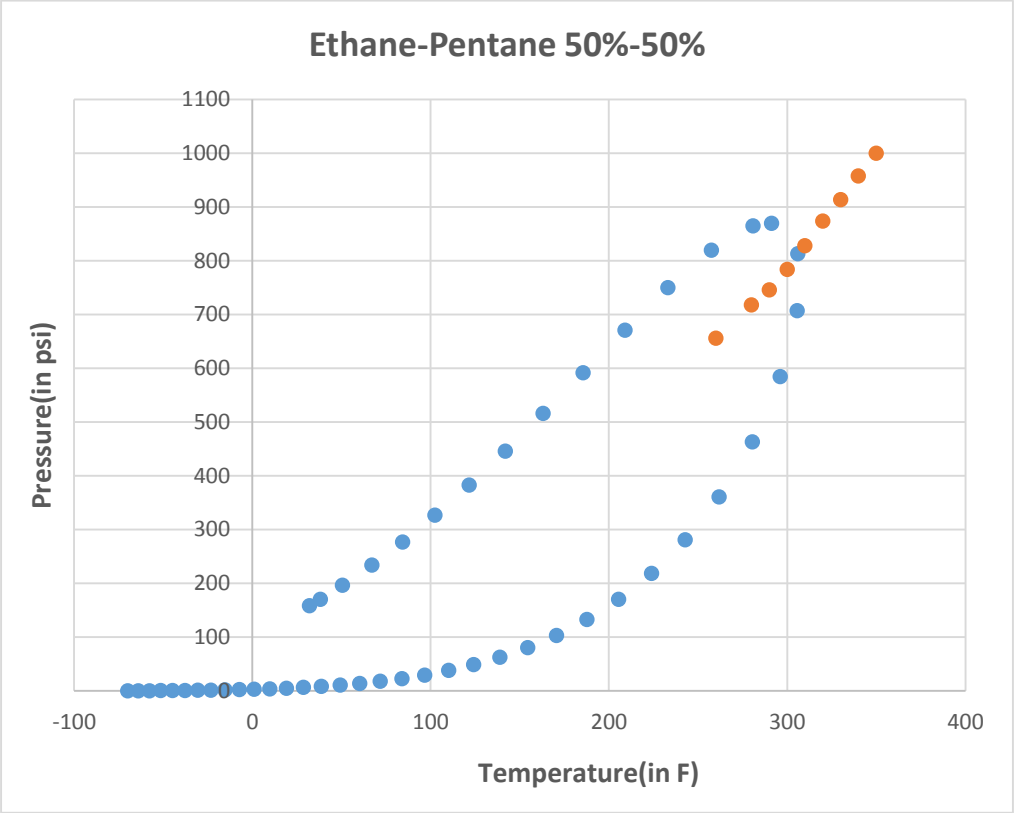

Figure 4.10: Two phase diagram of 50% Ethane – 50% Pentane with superimposed Pressure versus Temperature plot

2. Ethane 40% – Pentane 60%

The next step was to study the ethane-pentane in 40-60 mole percent composition. The phase diagram for this system is shown in Fig.4.11. Data from flash calculations of the z-factor for vapor phase, volume percent vapor and mole percent vapor are presented in tables 4.11, 4.12 and 4.13 as matrices respectively. The calculated number of moles and volume of the vapor phase are then presented in tables 4.14 and 4.15 respectively. The data for Pv/nz are shown in table 4.16 and then plotted in Fig. 4.12. The data for the calculated pressure as a function of temperature are then shown in table 4.17 and plotted in Fig.4.13.

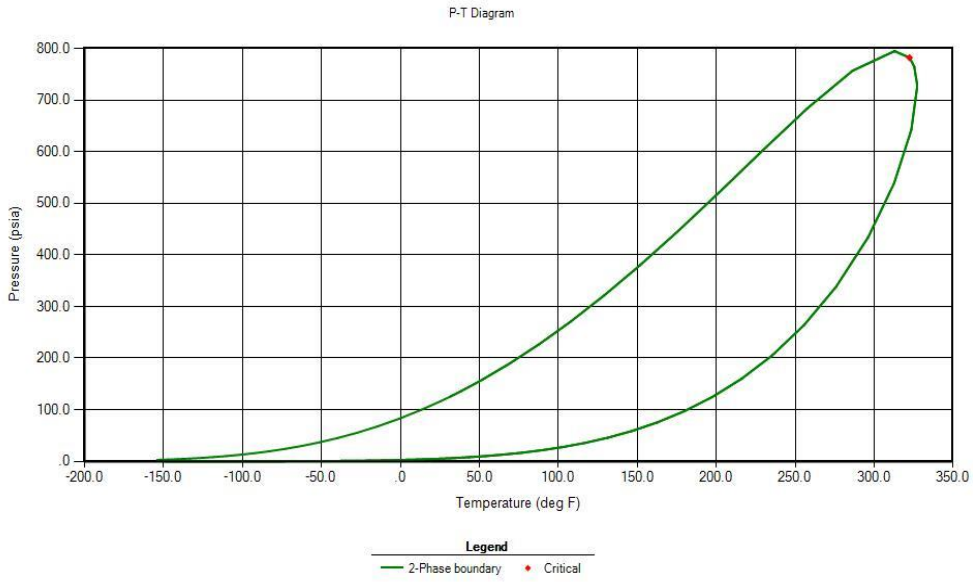

Figure 4.11: Two phase diagram of 50% Ethane – 50% Pentane

Table 4.11: Z-factor of 40% Ethane – 60% Pentane system

Z-factor for Gas											
Pressure	**1000**	**900**	**800**	**750**	**740**	**730**	**720**	**700**	**600**	**500**	**400**
Temperature											
350	0.4258	0.4499	0.5001	0.5332	0.5401	0.5472	0.5543	0.5686	0.6401	0.7085	0.7729
340	0.3971	0.4125	0.4586	0.4946	0.5024	0.5104	0.5185	0.5348	0.6159	0.6914	0.761
330	0.3715	0.3767	0.4113	0.4477	0.4564	0.4654	0.4746	0.4936	0.5879	0.6725	0.7481
320	0.3497	0.3458	0.3624	0.4614	0.4705	0.4787	0.4863	0.5001	0.5545	0.6512	0.734
310	0.3316	0.3210	0.3213	0.4952	0.5023	0.5089	0.5153	0.5271	0.5757	0.6269	0.7187
300	0.3167	0.3016	0.2917	0.5207	0.5269	0.5328	0.5385	0.5493	0.5956	0.6329	0.7017
280	0	0	0	0.2470	0.5631	0.5684	0.5735	0.5835	0.6278	0.6654	0.6974
260	0	0	0	0	0	0	0	0	0.6514	0.6903	0.7246
240	0	0	0	0	0	0	0	0	0.6676	0.7084	0.7453

Table 4.12: Vapor phase volume percent of 40% Ethane – 60% Pentane

Vapor Phase Volume %											
Pressure	**1000**	**900**	**800**	**750**	**740**	**730**	**720**	**700**	**600**	**500**	**400**
Temperature											
350	100	100	100	100	100	100	100	100	100	100	100
340	100	100	100	100	100	100	100	100	100	100	100
330	100	100	100	100	100	100	100	100	100	100	100
320	100	100	100	68.0866	72.5163	76.2107	79.3845	84.6406	100	100	100
310	100	100	100	45.7060	51.5072	56.5259	60.9306	68.3432	90.5452	100	100
300	100	100	100	28.9332	35.3566	41.0582	46.1604	54.9249	82.0455	95.9143	100
280	0	0	0	100	2.1313	9.6648	16.5019	28.4255	66.1517	85.4294	96.5565
260	0	0	0	0	0	0	0	0	48.3718	75.0849	89.7747
240	0	0	0	0	0	0	0	0	23.0338	63.0541	82.9528

Table 4.13: Vapor phase mol percent of 40% Ethane – 60% Pentane

Vapor Phase Mol %											
Pressure	**1000**	**900**	**800**	**750**	**740**	**730**	**720**	**700**	**600**	**500**	**400**
Temp.											
350	100	100	100	100	100	100	100	100	100	100	100
340	100	100	100	100	100	100	100	100	100	100	100
330	100	100	100	100	100	100	100	100	100	100	100
320	100	100	100	58.6971	62.5989	66.0218	69.1352	74.7971	100	100	100
310	100	100	100	32.6658	37.08	41.0287	44.6275	51.08	77.5254	100	100
300	100	100	100	17.4416	21.5447	25.3024	28.7817	35.0992	60.5802	85.8014	100
280	0	0	0	100	0.9368	4.3233	7.5114	13.3947	37.0515	57.7368	83.1937
260	0	0	0	0	0	0	0	0	20.6083	39.3909	59.0105
240	0	0	0	0	0	0	0	0	7.2212	25.7394	42.9546

Table 4.14: Number of moles in vapor phase of 40% Ethane – 60% Pentane system

n_g											
Pressure	**1000**	**900**	**800**	**750**	**740**	**730**	**720**	**700**	**600**	**500**	**400**
Temp.											
350	0.000239	0.000239	0.000239	0.000239	0.000239	0.000239	0.0002386	0.000239	0.000239	0.000239	0.000239
340	0.000239	0.000239	0.000239	0.000239	0.000239	0.000239	0.0002386	0.000239	0.000239	0.000239	0.000239
330	0.000239	0.000239	0.000239	0.000239	0.000239	0.000239	0.0002386	0.000239	0.000239	0.000239	0.000239
320	0.000239	0.000239	0.000239	0.00014	0.000149	0.000158	0.00016496	0.000178	0.000239	0.000239	0.000239
310	0.000239	0.000239	0.000239	7.79E-05	8.85E-05	9.79E-05	0.00010648	0.000122	0.000185	0.000239	0.000239
300	0.000239	0.000239	0.000239	4.16E-05	5.14E-05	6.04E-05	6.8673E-05	8.37E-05	0.000145	0.000205	0.000239
280	0	0	0	0.000239	2.24E-06	1.03E-05	1.7922E-05	3.2E-05	8.84E-05	0.000138	0.000198
260	0	0	0	0	0	0	0	0	4.92E-05	9.4E-05	0.000141
240	0	0	0	0	0	0	0	0	1.72E-05	6.14E-05	0.000102

Table 4.15: Vapor phase volume of 40% Ethane – 60% Pentane system

Vg											
Pressure	**1000**	**900**	**800**	**750**	**740**	**730**	**720**	**700**	**600**	**500**	**400**
Temp.											
350	0.000883	0.000883	0.000883	0.000883	0.000883	0.000883	0.000883	0.000883	0.000883	0.000883	0.000883
340	0.000883	0.000883	0.000883	0.000883	0.000883	0.000883	0.000883	0.000883	0.000883	0.000883	0.000883
330	0.000883	0.000883	0.000883	0.000883	0.000883	0.000883	0.000883	0.000883	0.000883	0.000883	0.000883
320	0.000883	0.000883	0.000883	0.000601	0.00064	0.000673	0.000701	0.000747	0.000883	0.000883	0.000883
310	0.000883	0.000883	0.000883	0.000403	0.000455	0.000499	0.000538	0.000603	0.000799	0.000883	0.000883
300	0.000883	0.000883	0.000883	0.000255	0.000312	0.000362	0.000408	0.000485	0.000724	0.000847	0.000883
280	0	0	0	0.000883	1.88E-05	8.53E-05	0.000146	0.000251	0.000584	0.000754	0.000852
260	0	0	0	0	0	0	0	0	0.000427	0.000663	0.000793
240	0	0	0	0	0	0	0	0	0.000203	0.000557	0.000732

Table 4.16: P^*v_g/Z^*n_g chart of 40% Ethane – 60% Pentane system

P^*v_g/Z^*n_g											
Pressure	**1000**	**900**	**800**	**750**	**740**	**730**	**720**	**700**	**600**	**500**	**400**
Temperature											
350	8689.3	7401.	5918.7	5204	5069.3	4935.9	4805.9	4554.9	3468.1	2611.1	1914.8
340	9317.3	8072.	6454.3	5610	5449.7	5291.8	5137.8	4842.8	3604.4	2675.6	1944.7
330	9959.4	8839.	7196.5	6198	5999.0	5803.5	5613.0	5247.0	3776.0	2750.8	1978.3
320	10580.0	9629.	8167.6	6976	6741.1	6513.0	6290.1	5860.4	4003.5	2840.8	2016.3
310	11157.0	10373	9212.4	7840	7571.6	7312.1	7058.2	6574.2	4503.7	2950.9	2059.2
300	11682	11040	10147	8840	8527.6	8226.0	7934.0	7378.2	5047.9	3267.5	2109.1
280	-	-	-	1123	11062.	10622.	10204.	9419.4	6313.3	4113.7	2462.9
260	-	-	-	-	-	-	-	-	7999.2	5108.3	3107.2

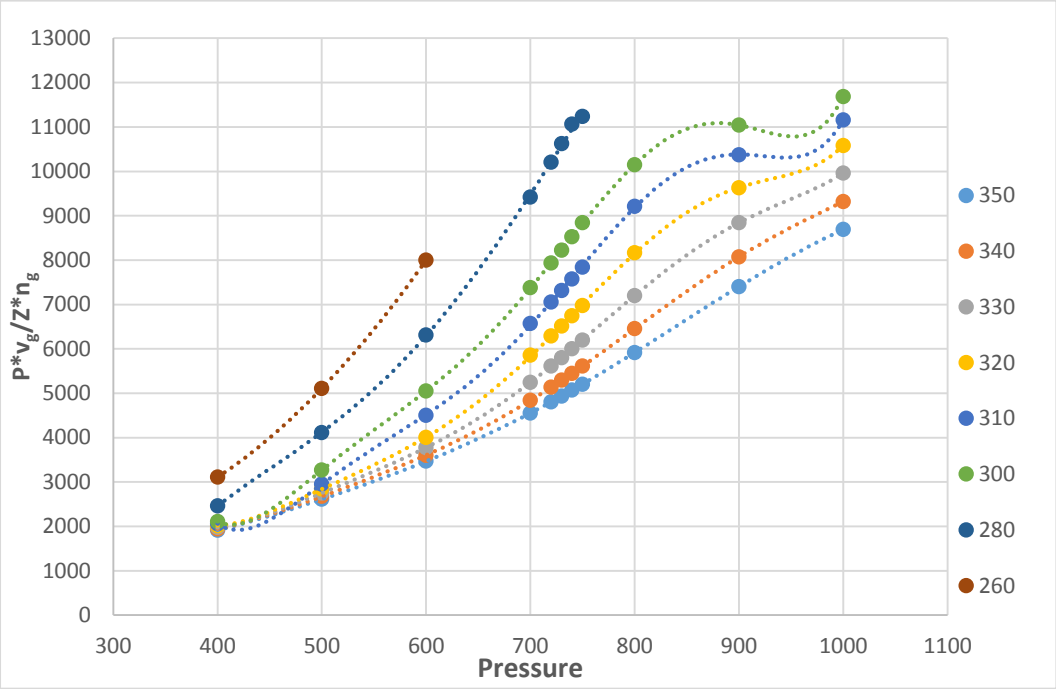

Figure 4.12: P^*v_g/Z^*n_g versus Pressure of 40% Ethane – 60% Pentane

Table 4.17: Pressure at each Temperature step for 40% Ethane – 60% Pentane

T(in F)	P (in psi)
350	1000
340	938
330	874
320	812
310	765
300	727
280	655
260	593

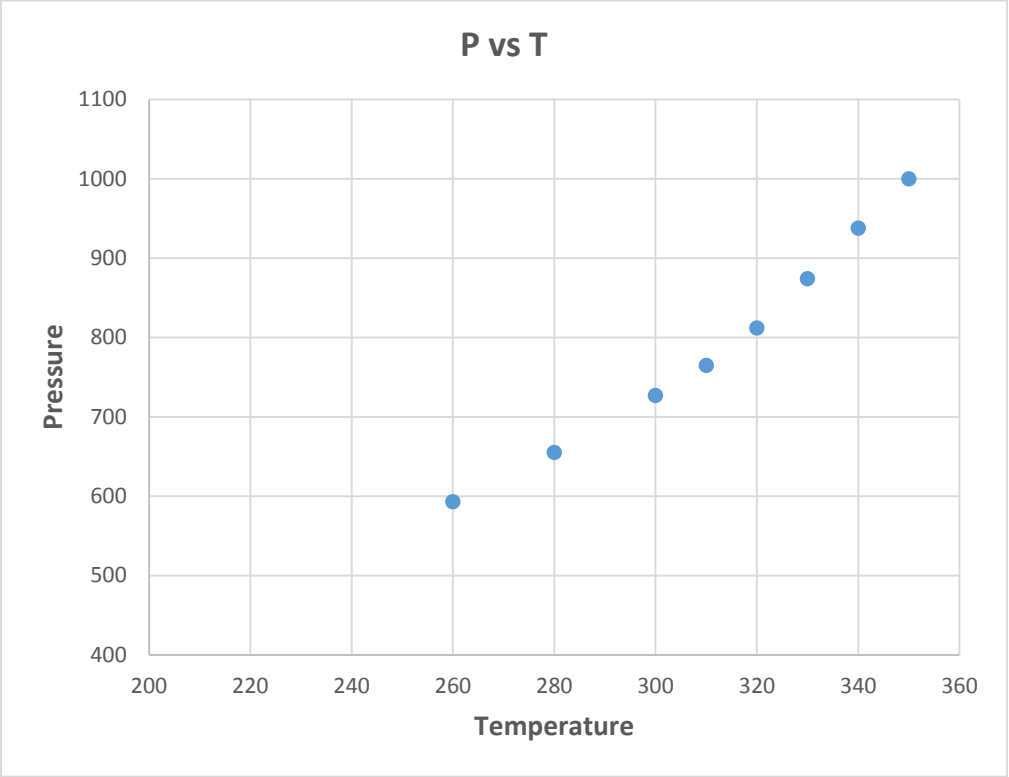

Figure 4.13: Pressure versus Temperature of 40% Ethane – 60% Pentane

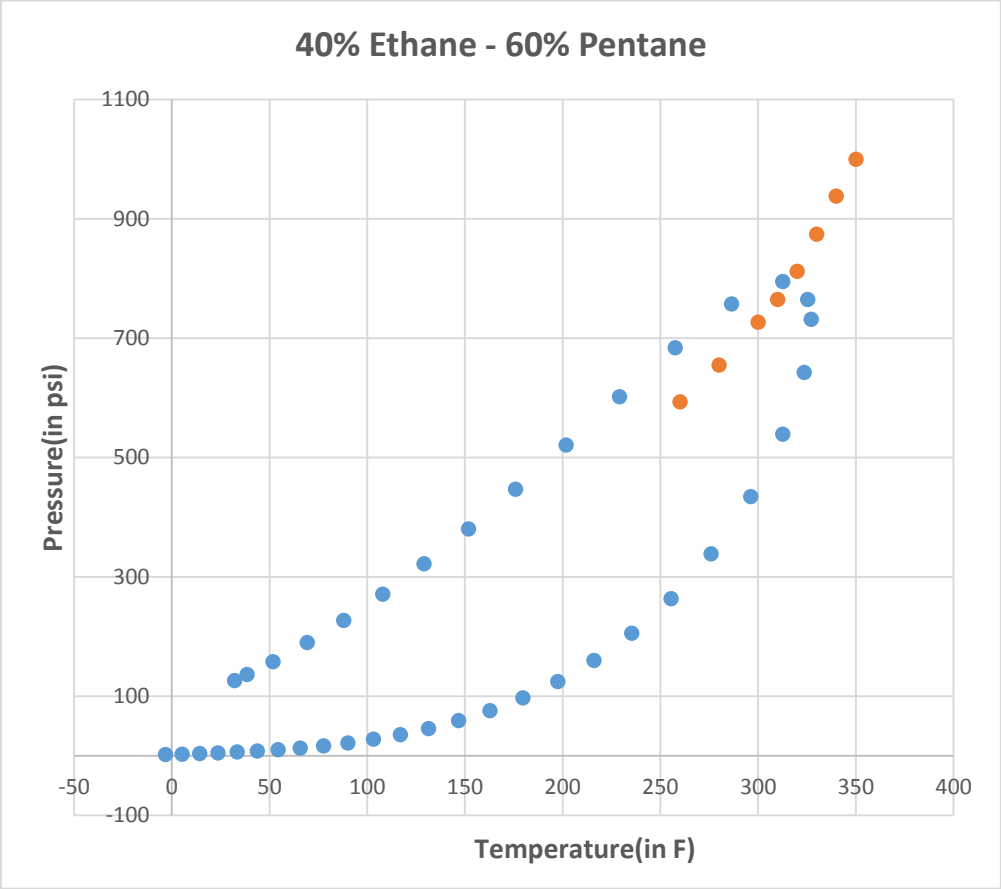

Figure 4.14: Two phase diagram of 40% Ethane – 60% Pentane with superimposed Pressure versus Temperature plot

3. Ethane 40% – Pentane 60% at Initial Pressure 800psi and Initial Temperature 350F.

The results for the 40-60 ethane-pentane system showed a lot of promise in terms of the change in slope as well as reasonable data ranges of temperature and pressure. We wanted to explore what would be the result of the starting point is modified. In this section we present the results for the system with a starting point of 350 F and

800 psi instead of 1000 psi. The detailed matrices are presented in Appendix D. Below we show the pressure/temperature data in table 4.18 and in Fig.4.16 overlapping the phase diagram.

Figure 4.18: Pressure at each Temperature step for 40% Ethane – 60% Pentane at initial pressure of 800psi

T(in F)	P (in psi)
340	764
330	728
320	693
310	657
300	625
280	563
260	507
240	456

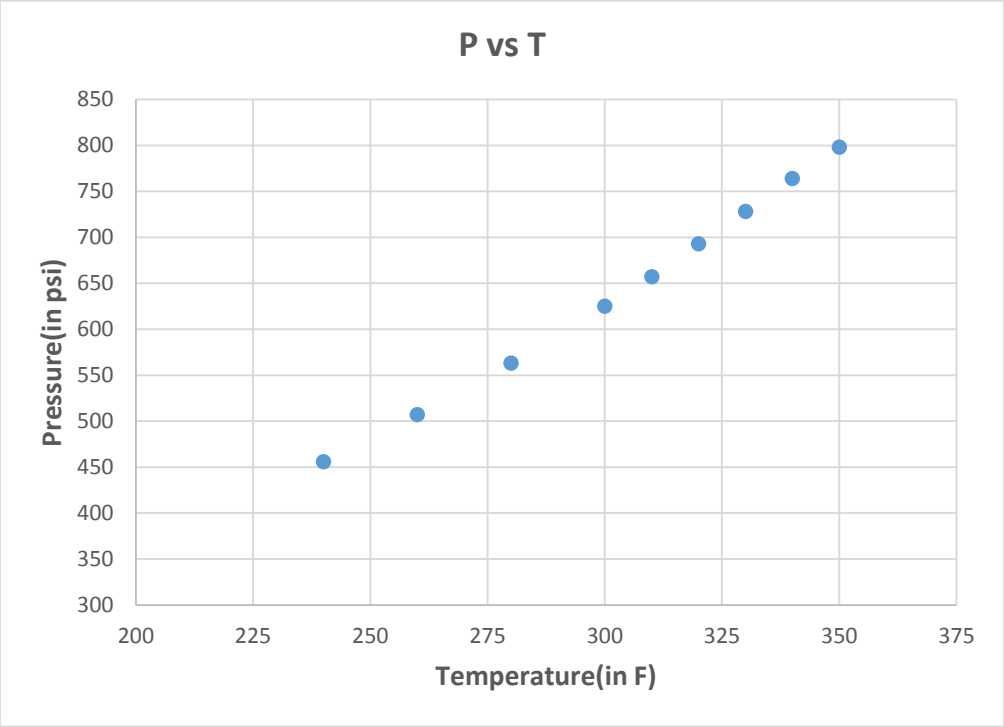

Figure 4.15: Pressure versus Temperature of 40% Ethane – 60% Pentane

40% Ethane – 60% Pentane (with initial pressure of 800psi and initial temperature of 350 F) phase envelope with superimposed P vs T plot:

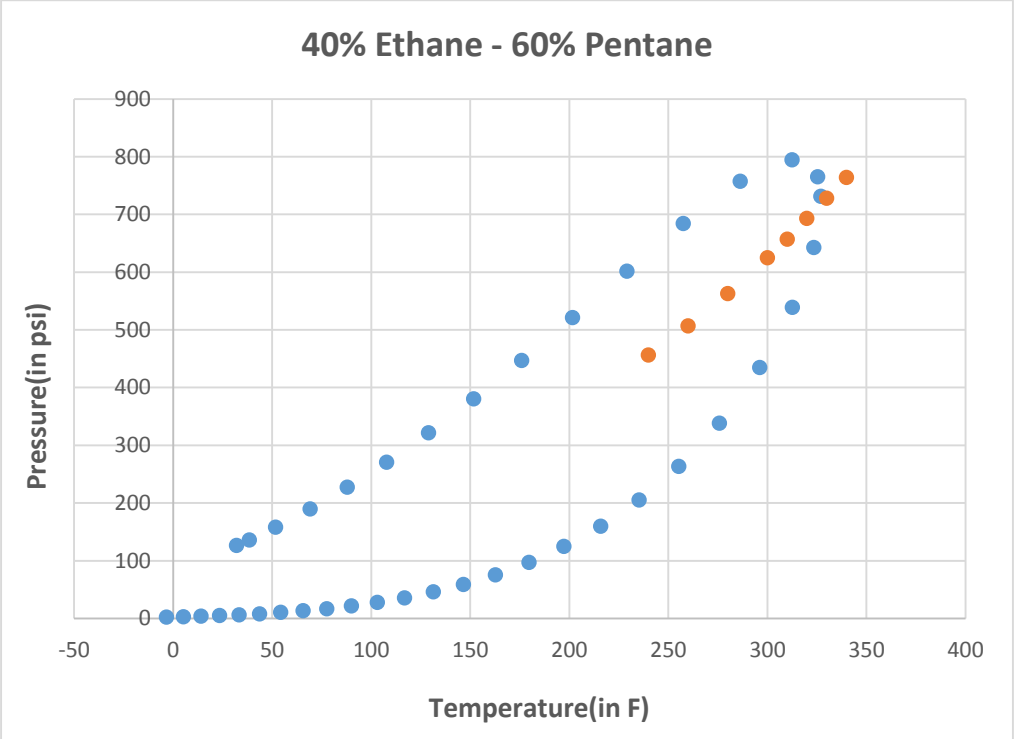

Figure 4.16: Two phase diagram of 40% Ethane – 60% Pentane at initial pressure of 800psi with superimposed Pressure versus Temperature plot

Table 4.19: Z-factor of 40% Ethane – 60% Pentane system at initial pressure of 800psi

Z-factor for Gas											
Pressure	**800**	**750**	**700**	**650**	**600**	**550**	**500**	**450**	**400**	**350**	**300**
Temperature											
350	0.5001	0.5332	0.5686	0.6046	0.6401	0.6748	0.7085	0.7412	0.7729	0.8037	0.8337
340	0.4586	0.4946	0.5348	0.5758	0.6159	0.6545	0.6914	0.7269	0.761	0.7939	0.8257
330	0.4113	0.4477	0.4936	0.5416	0.5879	0.6314	0.6725	0.7112	0.7481	0.7833	0.8172
320	0.3624	0.4614	0.5001	0.5289	0.5545	0.605	0.6512	0.694	0.734	0.772	0.8081
310	0.3213	0.4952	0.5271	0.5532	0.5757	0.5956	0.6269	0.6747	0.7187	0.7597	0.7983
300	0.2917	0.5207	0.5493	0.5738	0.5956	0.6151	0.6329	0.6531	0.7017	0.7463	0.7878
280	0.2558	0.247	0.5835	0.6066	0.6278	0.6473	0.6654	0.6821	0.6974	0.7156	0.7642
260	0	0	0	0.63	0.6514	0.6715	0.6903	0.708	0.7246	0.7399	0.7536
240	0	0	0	0	0.6676	0.6886	0.7084	0.7273	0.7453	0.7621	0.7778

Table 4.20: Vapor phase volume percent of 40% Ethane – 60% Pentane system at initial pressure of 800psi

Vapor Phase Volume %											
Pressure	**800**	**750**	**700**	**650**	**600**	**550**	**500**	**450**	**400**	**350**	**300**
Temperature											
350	100	100	100	100	100	100	100	100	100	100	100
340	100	100	100	100	100	100	100	100	100	100	100
330	100	100	100	100	100	100	100	100	100	100	100
320	100	68.0866	84.6406	93.9784	100	100	100	100	100	100	100
310	100	45.706	68.3432	81.6279	90.5452	96.9504	100	100	100	100	100
300	100	28.9332	54.9249	71.0466	82.0455	89.9782	95.9143	100	100	100	100
280	100	100	28.4255	50.7734	66.1517	77.2119	85.4294	91.6902	96.5565	100	100
260	0	0	0	26.1152	48.3718	63.8774	75.0849	83.4237	89.7747	94.7056	98.596
240	0	0	0	0	23.0338	46.8606	63.0541	74.5372	82.9528	89.2849	94.1526

Table 4.21: Vapor phase mole percent of 40% Ethane – 60% Pentane system at initial pressure of 800psi

Vapor Phase Mol %											
Pressure	**800**	**750**	**700**	**650**	**600**	**550**	**500**	**450**	**400**	**350**	**300**
Temp.											
350	100	100	100	100	100	100	100	100	100	100	100
340	100	100	100	100	100	100	100	100	100	100	100
330	100	100	100	100	100	100	100	100	100	100	100
320	100	58.6971	74.7971	87.6465	100	100	100	100	100	100	100
310	100	32.6658	51.08	64.8486	77.5254	90.8895	100	100	100	100	100
300	100	17.4416	35.0992	48.5823	60.5802	72.5505	85.8014	100	100	100	100
280	100	100	13.3947	26.0738	37.0515	47.3332	57.7368	69.2003	83.1937	100	100
260	0	0	0	9.9659	20.6083	30.2152	39.3909	48.73	59.0105	71.5603	89.2842
240	0	0	0	0	7.2212	16.8773	25.7394	34.2641	42.9546	52.5333	64.3386

Table for number of moles and volume of vapor phase at each pressure temperature step:

Table 4.22: Number of moles in vapor phase of 40% Ethane – 60% Pentane system at initial pressure of 800psi

Pressure	800	750	700	650	600	550	500	450	400	350	300
Temp.											
350	0.000163	0.000163	0.000163	0.000163	0.000163	0.000163	0.00016256	0.000163	0.000163	0.000163	0.000163
340	0.000163	0.000163	0.000163	0.000163	0.000163	0.000163	0.00016256	0.000163	0.000163	0.000163	0.000163
330	0.000163	0.000163	0.000163	0.000163	0.000163	0.000163	0.00016256	0.000163	0.000163	0.000163	0.000163
320	0.000163	9.54E-05	0.000122	0.000142	0.000163	0.000163	0.00016256	0.000163	0.000163	0.000163	0.000163
310	0.000163	5.31E-05	8.3E-05	0.000105	0.000126	0.000148	0.00016256	0.000163	0.000163	0.000163	0.000163
300	0.000163	2.84E-05	5.71E-05	7.9E-05	9.85E-05	0.000118	0.00013948	0.000163	0.000163	0.000163	0.000163
280	0.000163	0.000163	2.18E-05	4.24E-05	6.02E-05	7.69E-05	9.3855E-05	0.000112	0.000135	0.000163	0.000163
260	0	0	0	1.62E-05	3.35E-05	4.91E-05	6.4033E-05	7.92E-05	9.59E-05	0.000116	0.000145
240	0	0	0	0	1.17E-05	2.74E-05	4.1841E-05	5.57E-05	6.98E-05	8.54E-05	0.000105

Table 4.23: Vapor phase volume of 40% Ethane – 60% Pentane system at initial pressure of 800psi

V_g											
Pressure	**800**	**750**	**700**	**650**	**600**	**550**	**500**	**450**	**400**	**350**	**300**
Temperature											
350	0.00088	0.00088	0.00088	0.00088	0.00088	0.00088	0.00088	0.00088	0.00088	0.00088	0.00088
340	0.00088	0.00088	0.00088	0.00088	0.00088	0.00088	0.00088	0.00088	0.00088	0.00088	0.00088
330	0.00088	0.00088	0.00088	0.00088	0.00088	0.00088	0.00088	0.00088	0.00088	0.00088	0.00088
320	0.00088	0.00060	0.00074	0.00083	0.00088	0.00088	0.00088	0.00088	0.00088	0.00088	0.00088
310	0.00088	0.00040	0.00060	0.00072	0.0008	0.00085	0.00088	0.00088	0.00088	0.00088	0.00088
300	0.00088	0.00025	0.00048	0.00062	0.00072	0.00079	0.00084	0.00088	0.00088	0.00088	0.00088
280	0.00088	0.00088	0.00025	0.00044	0.00058	0.00068	0.00075	0.00081	0.00085	0.00088	0.00088
260	0	0	0	0.00023	0.00042	0.00056	0.00066	0.00073	0.00079	0.00083	0.00087
240	0	0	0	0	0.00020	0.00041	0.00055	0.00065	0.00073	0.00078	0.00083

Table 4.24: P^*v_g/Z^*n_g chart of 40% Ethane – 60% Pentane system at initial pressure of 800psi

P^*v_g/Z^*n_g											
Pressure	**800**	**750**	**700**	**650**	**600**	**550**	**500**	**450**	**400**	**350**	**300**
Temperature											
350	8689.3	7640.58	6687.23	5839.83	5091.65	4427.34	3833.41	3297.86	2811.20	2365.53	1954.64
340	9475.7	8236.88	7109.87	6131.93	5291.71	4564.66	3928.22	3362.74	2855.16	2394.73	1973.57
330	10565.4	9099.75	7703.32	6519.14	5543.74	4731.66	4038.62	3436.97	2904.39	2427.14	1994.10
320	11991	10241.9	8603.80	7157.95	5877.67	4938.13	4170.72	3522.15	2960.18	2462.67	2016.56
310	13524	11511.0	9651.72	8033.87	6611.98	5350.56	4332.38	3622.90	3023.20	2502.54	2041.31
300	14897	12978.9	10832.1	8998.57	7410.99	6023.78	4797.10	3742.72	3096.45	2547.47	2068.52
280	16988	16493.7	13828.9	11334.4	9268.74	7528.89	6039.45	4748.26	3615.96	2656.76	2132.40
260	-	-	-	14686.0	11743.8	9405.76	7499.70	5910.55	4561.86	3400.58	2387.92
240	-	-	-	-	15572.0	12046.3	9392.08	7311.19	5629.96	4239.89	3065.98

P*V/z*n vs. P plots:

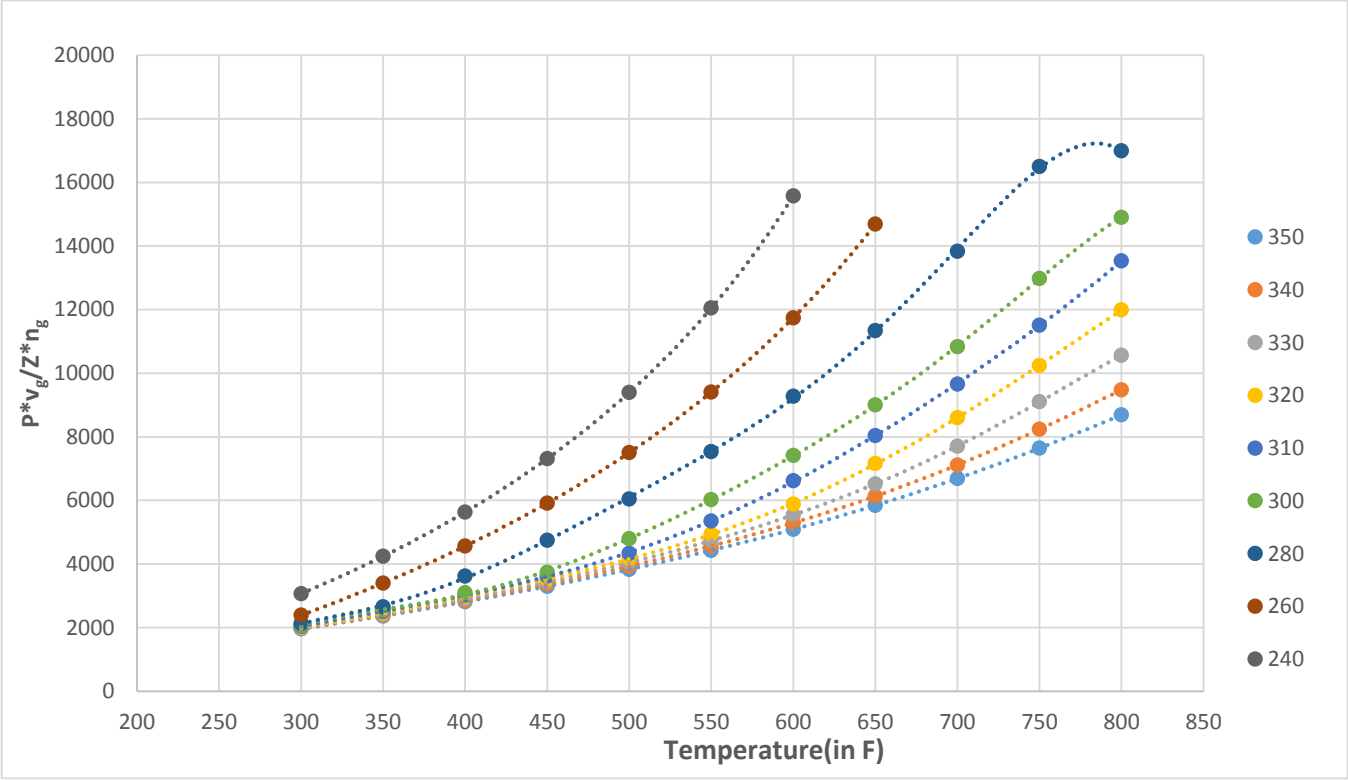

Figure 4.17: $P*v_g/Z*n_g$ versus Pressure of 40% Ethane – 60% pentane at initial pressure of 800 psi

4. Ethane 40% – Pentane 60% at Initial T = 350F and Initial P = 600psi

Further changing the starting point down to 600 psi changes the slope and the expected experimental results further. The details of the row data are presented in Appendix E. Below are the pressure-temperature values shown in table 4.25 and in Fig.4.18.

Table 4.25: Pressure at each Temperature step for 40% Ethane – 60% Pentane at initial pressure of 600psi

T(in F)	P (in psi)
340	583
330	566
320	548
310	526
300	499
280	446
260	398
240	357

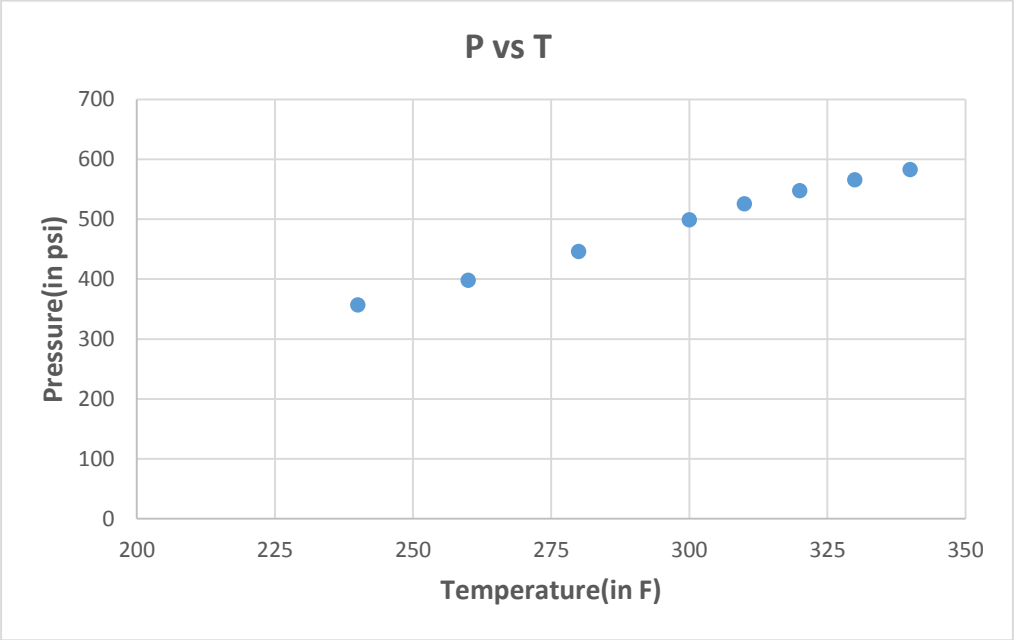

Figure 4.18: Pressure versus Temperature of 40% Ethane – 60% Pentane at initial pressure of 600psi

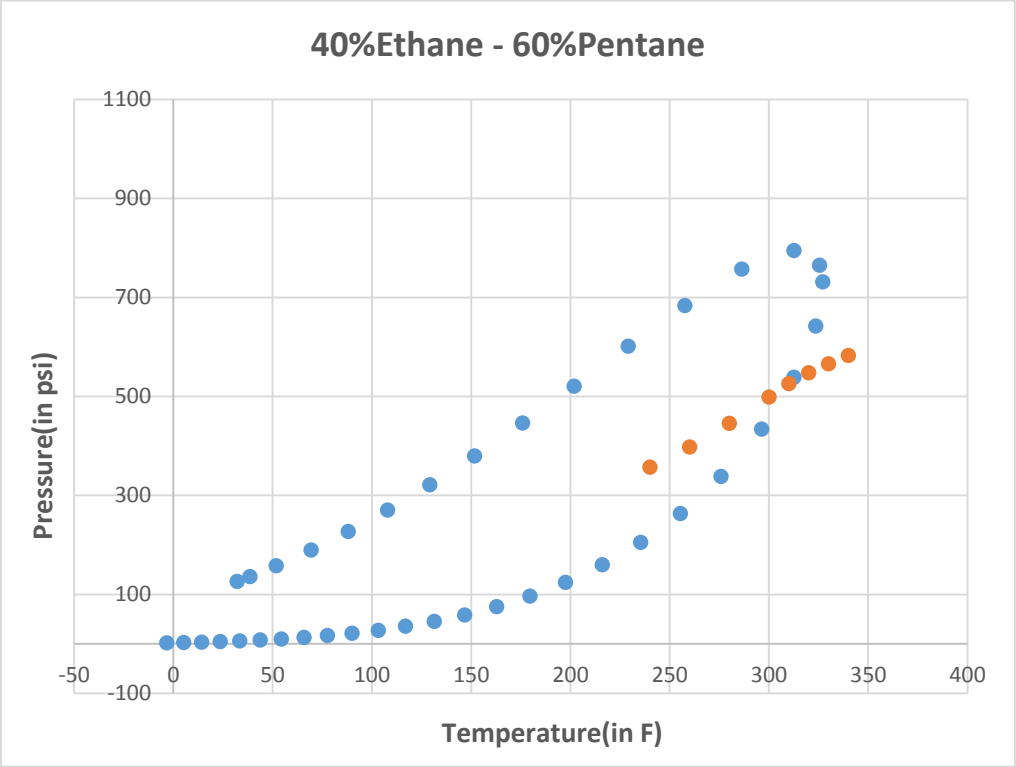

Figure 4.19: Two phase diagram of 40% Ethane – 60% Pentane at initial pressure of 600psi with superimposed Pressure versus Temperature plot

Table 4.26: Z-factor of 40% Ethane – 60% Pentane at initial pressure system of 600psi

Z-factor for GAS							
Pressure	**600**	**550**	**500**	**450**	**400**	**350**	**300**
Temperature							
350	0.6401	0.6748	0.7085	0.7412	0.7729	0.8037	0.8337
340	0.6159	0.6545	0.6914	0.7269	0.761	0.7939	0.8257
330	0.5879	0.6314	0.6725	0.7112	0.7481	0.7833	0.8172
320	0.5545	0.605	0.6512	0.694	0.734	0.772	0.8081
310	0.5757	0.5956	0.6269	0.6747	0.7187	0.7597	0.7983
300	0.5956	0.6151	0.6329	0.6531	0.7017	0.7463	0.7878
280	0.6278	0.6473	0.6654	0.6821	0.6974	0.7156	0.7642
260	0.6514	0.6715	0.6903	0.708	0.7246	0.7399	0.7536
240	0.6676	0.6886	0.7084	0.7273	0.7453	0.7621	0.7778

Table 4.27: Vapor phase volume percent of 40% Ethane – 60%

Pentane system at initial pressure of 600psi

Vapor Phase Volume %							
Pressure	**600**	**550**	**500**	**450**	**400**	**350**	**300**
Temperature							
350	100	100	100	100	100	100	100
340	100	100	100	100	100	100	100
330	100	100	100	100	100	100	100
320	100	100	100	100	100	100	100
310	90.5452	96.9504	100	100	100	100	100
300	82.0455	89.9782	95.9143	100	100	100	100
280	66.1517	77.2119	85.4294	91.6902	96.5565	100	100
260	48.3718	63.8774	75.0849	83.4237	89.7747	94.7056	98.596
240	23.0338	46.8606	63.0541	74.5372	82.9528	89.2849	94.1526

Table 4.28: Vapor phase mol percent of 40% Ethane – 60% Pentane system at initial pressure of 600psi

Vapor Phase Mol %							
Pressure	**600**	**550**	**500**	**450**	**400**	**350**	**300**
Temperature							
350	100	100	100	100	100	100	100
340	100	100	100	100	100	100	100
330	100	100	100	100	100	100	100
320	100	100	100	100	100	100	100
310	77.5254	90.8895	100	100	100	100	100
300	60.5802	72.5505	85.8014	100	100	100	100
280	37.0515	47.3332	57.7368	69.2003	83.1937	100	100
260	20.6083	30.2152	39.3909	48.73	59.0105	71.5603	89.2842
240	7.2212	16.8773	25.7394	34.2641	42.9546	52.5333	64.3386

Table 4.29: Number of moles in vapor phase of 40% Ethane – 60% Pentane system at initial pressure of 600psi

n_g							
Pressure	**600**	**550**	**500**	**450**	**400**	**350**	**300**
Temp.							
350	9.53E-05	9.53E-05	9.53E-05	9.53E-05	9.53E-05	9.53E-05	9.5252E-05
340	9.53E-05	9.53E-05	9.53E-05	9.53E-05	9.53E-05	9.53E-05	9.5252E-05
330	9.53E-05	9.53E-05	9.53E-05	9.53E-05	9.53E-05	9.53E-05	9.5252E-05
320	9.53E-05	9.53E-05	9.53E-05	9.53E-05	9.53E-05	9.53E-05	9.5252E-05
310	7.38E-05	8.66E-05	9.53E-05	9.53E-05	9.53E-05	9.53E-05	9.5252E-05
300	5.77E-05	6.91E-05	8.17E-05	9.53E-05	9.53E-05	9.53E-05	9.5252E-05
280	3.53E-05	4.51E-05	5.5E-05	6.59E-05	7.92E-05	9.53E-05	9.5252E-05
260	1.96E-05	2.88E-05	3.75E-05	4.64E-05	5.62E-05	6.82E-05	8.5045E-05
240	6.88E-06	1.61E-05	2.45E-05	3.26E-05	4.09E-05	5E-05	6.1284E-05

Table 4.30: Vapor phase volume of 40% Ethane – 60% Pentane system at initial pressure of 600psi

Vg							
Pressure	**600**	**550**	**500**	**450**	**400**	**350**	**300**
Temp.							
350	0.000883	0.000883	0.000883	0.000883	0.000883	0.000883	0.000883
340	0.000883	0.000883	0.000883	0.000883	0.000883	0.000883	0.000883
330	0.000883	0.000883	0.000883	0.000883	0.000883	0.000883	0.000883
320	0.000883	0.000883	0.000883	0.000883	0.000883	0.000883	0.000883
310	0.0008	0.000856	0.000883	0.000883	0.000883	0.000883	0.000883
300	0.000724	0.000795	0.000847	0.000883	0.000883	0.000883	0.000883
280	0.000584	0.000682	0.000754	0.00081	0.000853	0.000883	0.000883
260	0.000427	0.000564	0.000663	0.000737	0.000793	0.000836	0.000871
240	0.000203	0.000414	0.000557	0.000658	0.000732	0.000788	0.000831

Table 4.31: P^*v_g/Z^*n_g chart of 40% Ethane – 60% Pentane system at initial pressure of 600psi

P*vg/Z*ng							
Pressure	**600**	**550**	**500**	**450**	**400**	**350**	**300**
Temp.							
350	8689.378	7555.669	6542.074	5628.108	4797.577	4037.006	3335.775
340	9030.802	7790.016	6703.875	5738.827	4872.598	4086.839	3368.094
330	9460.914	8075.016	6892.281	5865.514	4956.62	4142.144	3403.127
320	10030.79	8427.381	7117.72	6010.884	5051.836	4202.774	3441.45
310	11283.96	9131.228	7393.618	6182.827	5159.381	4270.819	3483.697
300	12647.54	10280.14	8186.706	6387.312	5284.377	4347.503	3530.129
280	15817.96	12848.75	10306.88	8103.352	6170.984	4534.016	3639.146
260	20041.9	16051.8	12798.94	10086.9	7785.233	5803.417	4075.213
240	26575.19	20558.24	16028.45	12477.22	9608.056	7235.769	5232.38

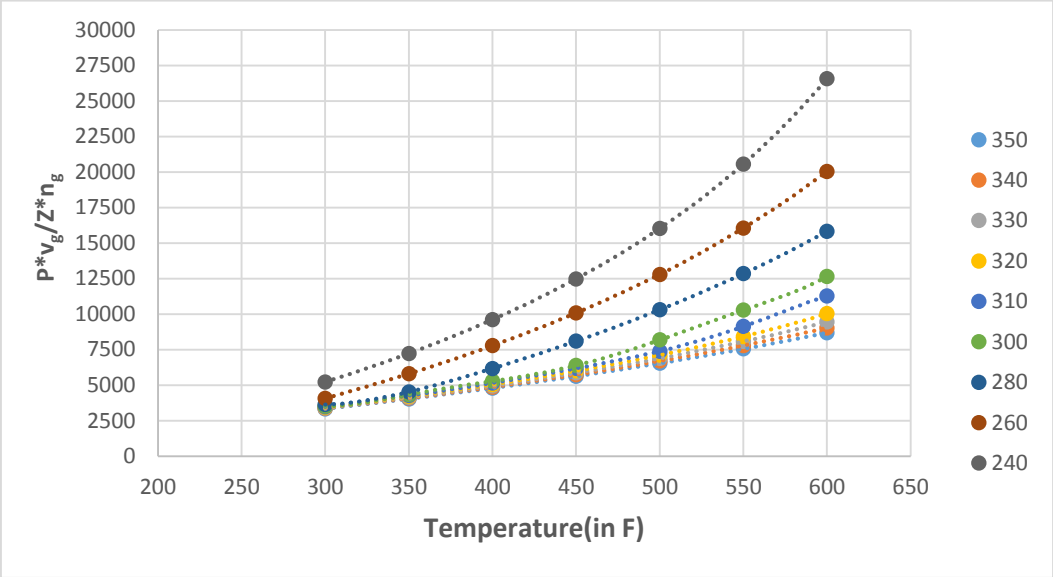

Figure 4.20: $P*v_g/Z*n_g$ versus Pressure of 40% Ethane – 60% Pentane at initial pressure of 600psi

4.3 SENSITIVITY OF RESULTS TO EQUATION OF STATE CHOICE

To check the sensitivity of results obtained by running simulations of various binary hydrocarbon system, Soave-Redlich Kwong (SRK) equation of state (EOS) was used for ethane-pentane system for 40% and 60% mol fractions. The initial conditions were considered same i.e., 1000 psi pressure and 350 F temperature.

The two-phase envelope for this system using SRK EOS is given in Fig. 4.21. The pressure corresponding to each Temperature step came out to be similar to the pressure values obtained using Peng-Robinson equation of state. Table 4.32

represents the pressure and corresponding temperature values and Fig. 4.22 Pressure versus Temperature plot.

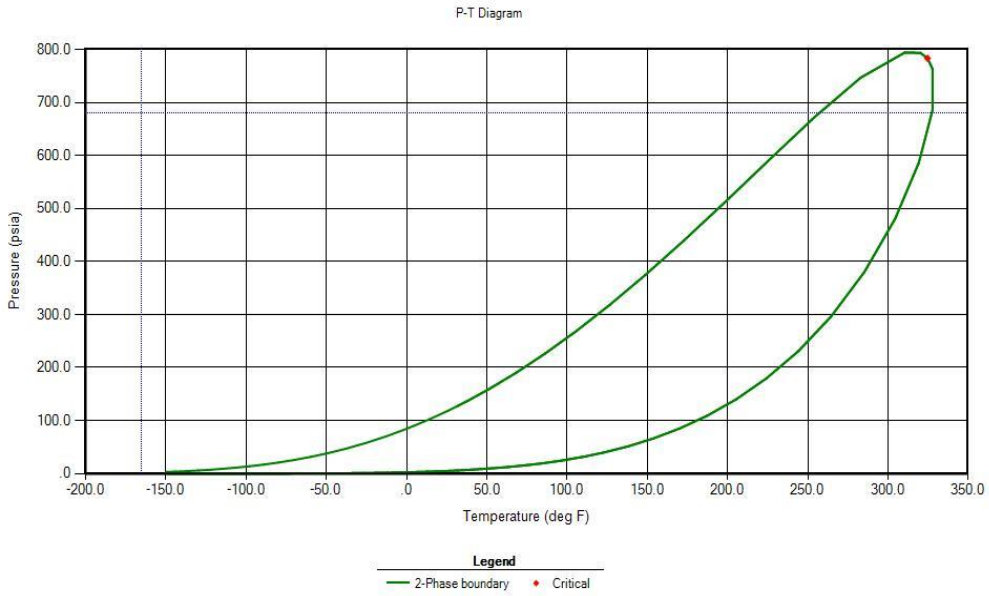

Figure 4.21: Two-phase diagram of 40% Ethane – 60% Pentane using SRK equation of state

Table 4.32: Pressure at each Temperature step for 40% Ethane – 60% Pentane using SRK equation of state

P (in psi)	T
1000	350
937	340
874	330
810	320
765	310
727	300
658	280
593	260

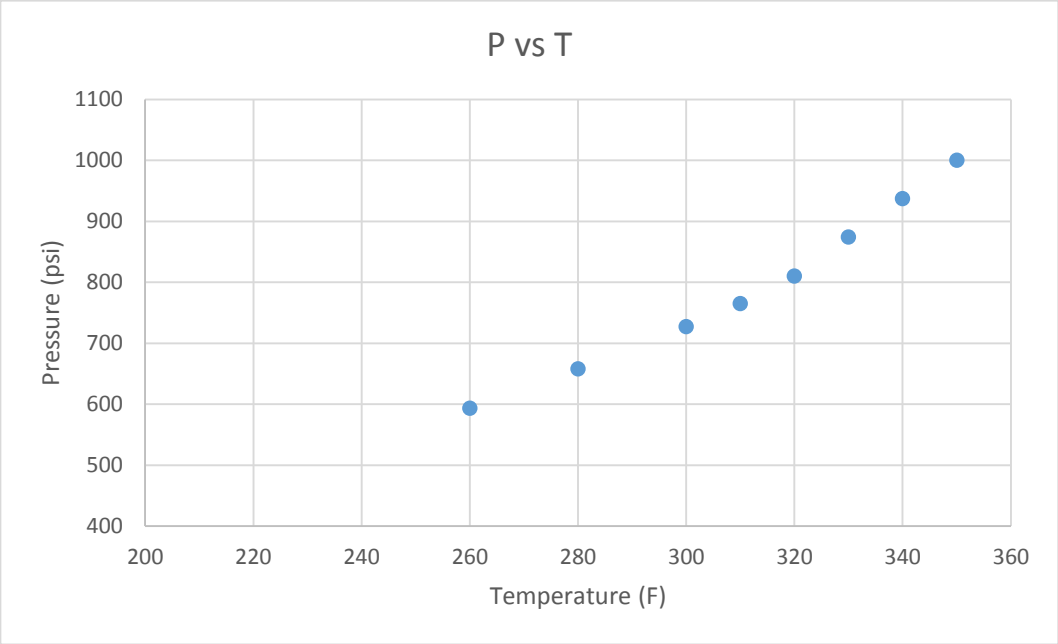

Figure 4.22: Pressure versus Temperature for 40% Ethane – 60% Pentane using SRK equation of state

To compare the sensitivity of using different equation of states and comparison, an overlapped plot using both equation of states is shown in Fig. 4.23. It is observed that two-phase envelope and the pressure change with the temperature for both the equations of states is almost identical and hence, can be used for further experiments.

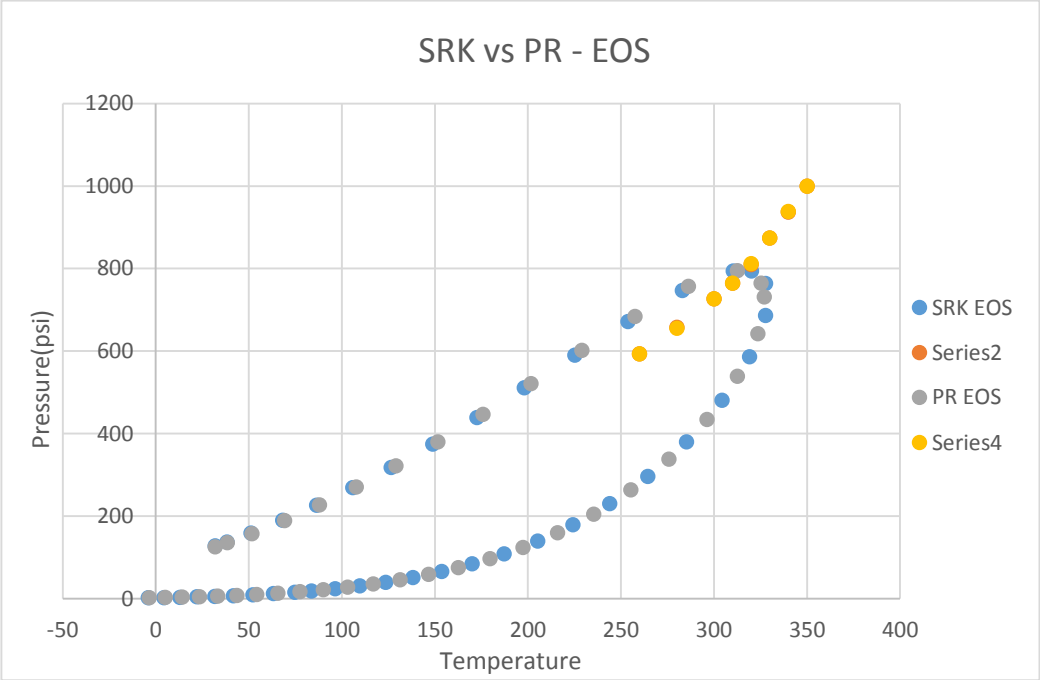

Figure 4.23: Two phase diagram of 40% Ethane – 60% Pentane superimposed Pressure versus Temperature plot using SRK and PR equation of states

CHAPTER 5: CONCLUSION AND RECOMMENDATION

5.1 Conclusion

From the simulation results presented in this thesis, we conclude:

- It is possible to conduct constant-volume, constant-composition experiments through which the edge of the phase diagram for some systems can be detected. This type of experiment would be the only type possible to be conducted under confinement conditions.
- The ethane-pentane system showed to be the most promising as a first test to analyze using this approach as the temperature and pressure conditions seem to be reasonable compared to experimental limitations and the change in slope as the system transitions from one to two phases is significant.
- The choice of 40 mole percent ethane ad 60 mole percent pentane with a starting point of 350 F and 1000 psi would be a good system to test to reproduce the results in bulk experimentally followed by experiments under confinement where results are expected to show a change in the location of the edge of phase envelope.

5.2 Recommendation

- This work can be extended to test the behavior in multi-component systems to study the viability of this approach.
- The work for two-component systems can be conducted under tight confinement. An experimental design is being put together by other members of the research team for this purpose.
- The extension of this work should also include the effect of non-hydrocarbon impurities on altering the phase behavior.
- Further analysis should take the mobility and dynamic testing into account.

REFERENCES

Ahmed, Tarek 2007. On Equation of State. Paper SPE-107331 presented at the SPE Latin American and Caribbean Petroleum Engineering Conference, Buenos Aires, Argentina, 15-18 April 2007.

Akkutlu, I.Y., Rahmani Didar, B. 2013. Pore-size Dependence of Fluid Phase Behavior and the Impact on Shale Gas Reserves. Paper SPE-168939/ URTeC 1624453 presented at the Unconventional Resources Technology Conference, Denver, Colorado, USA, 12-14 August 2013.

Devegowda, D., Sapmanee, K., Civan, F. and Sigal, R. 2012. Phase Behavior of Gas Condensates in Shales Due to Pore Proximity Effects: Implications for Transport, Reserves and Well Productivity. Paper SPE-160099 presented at the SPE Annual Technical Conference and Exhibition, San Antonio, Texas, USA, 8-10 October 2012.

Firincioglu, T., Ozgen, C. NITEC LLC and Ozkan, E. SPE Colorado School of Mines 2012. Thermodynamics of Multiphase Flow in Unconventional Liquids-Rich Reservoirs. Paper SPE – 159869 presented at the SPE Annual Technical Conference and Exhibition, San Antonio, Texas, USA, 8-10 October 2012.

Firoozabadi, A. and Jin, Z., Reservoir Engineering Research Institute and Yale University 2015. Phase Behavior and Flow in Shale Nanopores From Molecular Simulations. Paper SPE-175151-MS presented at the SPE Annual Technical Conference and Exhibition, Houston, Texas, USA, 28-30 September 2015.

Jin, L., Ma, Yixin, Jamili, Ahmad, University of Oklahoma 2013. Investigating the effect of Pore Proximity on Phase Behavior and Fluid Properties in Shale Formations. Paper SPE-166192 presented at the SPE Annual Technical Conference and Exhibition, New Orleans, Louisiana, USA, 30 September-2 October 2013.

Kuila, U. and Prasad, M. Colorado School of Mines 2011. Surface Area and Pore-size Distribution in Clays and Shales. Paper SPE-146869 presented at the SPE Annual Technical Conference and Exhibition, Denver, Colorado, USA, 30 October – 2 November 2011.

Nojabaei, B., Johns, R. T., Pennsylvania State University and Chu, L. 2013. Effect of capillary pressure on phase behavior in tight rocks and shales. Paper SPE-159258 presented at the SPE Annual Technical Conference and Exhibition, San Antonio, Texas, USA, 8-10 October 2012.

Shapiro, A. A., & Stenby, E. H. 1996. Effects of Capillary Forces and Adsorption on Reserves Distribution. Paper SPE-36922 presented at the SPE European Petroleum Conference, Milan, Italy, 22-24 October 1996.

Sherborne, J. E. 1940, January 1. Fundamental Phase Behavior of Hydrocarbons. Society of Petroleum Engineers.

Sigmund, P. M., Dranchuk, P. M., Morrow, N. R., & Purvis, R. A. 1973. Retrograde Condensation in Porous Media. Paper SPE-3476-PA presented at SPE-AIME 46th Annual Fall Meeting, New Orleans, Louisiana, USA, 3-6 October 1971.

Standing, M.B. 1981. Volumetric and Phase Behavior of Oil Field Hydrocarbon Systems, ninth edition. Richardson, Texas: Society of Petroleum Engineers of AIME.

Udell, K.S. University of California 1982. The Thermodynamics of Evaporation and Condensation in Porous Media. Paper SPE – 10779 presented at the SPE

California Regional Meeting, San Francisco, California, USA, 24-26 March 1982.

Wang, L., Neeves, K.B., Yin, X. and Ozkan, E. 2014. Experimental Study and Modelling of the Effect of Pore Size Distribution on Hydrocarbon Phase Behavior in Nanopores. Paper SPE-170894-MS presented at the SPE Annual Technical Conference and Exhibition, Amsterdam, The Netherlands, 27-29 October 2014.

[1]McCain, Willian D. 1990 The properties of Petroleum Fluids, Second Edition. *PennWell Publishing Company, Tulsa, Oklahoma*. ISBN 0-87814-335-1

[2]Danesh, A. 2003. PVT and Phase Behavior of Petroleum Reservoir Fluids, third impression. *Elsevier Science B.V.* ISBN 0-444-82196-1

[3]Sengers, J. and Goodwin, A.R. and Peters, C. 2010. Applied Thermodynamics of Fluids. *Royal Society of Chemistry, 1st edition.* ISBN 978-1-84973-098-3

APPENDIX: NOMENCLATURE

SYMBOLS

a	attraction parameter of Van der Waals equation
b	repulsion parameter of Van der Waals equation
n	number of moles
n_g	number of moles of gas
P_c	critical pressure, dimensionless
R	universal gas constant
T_c	critical temperature, dimensionless
T_r	reduced temperature, dimensionless
V_b	volume at bubble point
V_m	molar volume
V_t	total volume in the cell
V_{sat}	saturated volume of liquid
V_o	remaining volume of liquid in cell
Z	compressibility factor, dimensionless

GREEK SYMBOLS

α	general function of Redlich-Kwong equation
∂	differentiation parameter
ω	accentric factor

APPENDIX A: Ethane – Butane System

Z-factor for GAS									
Pressure	**900**	**800**	**700**	**600**	**500**	**400**	**300**	**200**	**100**
Temperature									
300	0.5972	0.6419	0.6886	0.7357	0.7822	0.8278	0.8723	0.9158	0.9584
260	0.453	0.5203	0.594	0.6638	0.7284	0.7886	0.8452	0.899	0.9505
245	0.376	0.4441	0.5404	0.6269	0.7025	0.7705	0.8331	0.8916	0.9471
230	0.3117	0.3368	0.4878	0.58	0.672	0.75	0.8196	0.8835	0.9434
215	0.2737	0.2656	0.5097	0.5712	0.6346	0.7263	0.8045	0.8746	0.9393
200	0	0	0.5241	0.5861	0.6378	0.6985	0.7874	0.8648	0.9349
185	0	0	0	0.596	0.6501	0.6975	0.768	0.8539	0.9301
170	0	0	0	0	0.6581	0.7086	0.7535	0.8417	0.9249
140	0	0	0	0	0	0.7198	0.7724	0.8192	0.9127
110	0	0	0	0	0	0	0.7782	0.8345	0.8977
80	0	0	0	0	0	0	0	0.8385	0.8988
50	0	0	0	0	0	0	0	0.8318	0.9052

Vapor Phase Mol %									
Pressure	**900**	**800**	**700**	**600**	**500**	**400**	**300**	**200**	**100**
Temperature									
300	100	100	100	100	100	100	100	100	100
260	100	100	100	100	100	100	100	100	100
245	100	100	100	100	100	100	100	100	100
230	100	100	87.1686	100	100	100	100	100	100
215	100	100	42.2145	76.4432	100	100	100	100	100
200	0	0	8.2123	47.0714	76.4469	100	100	100	100
185	0	0	0	22.3678	52.6537	81.7537	100	100	100
170	0	0	0	0	32.4532	60.1802	94.022	100	100
140	0	0	0	0	0	26.0815	54.3024	93.3528	100
110	0	0	0	0	0	0	25.5939	56.6096	100
80	0	0	0	0	0	0	0	31.7645	73.1842
50	0	0	0	0	0	0	0	1.0665	47.7757

Vapor Phase Volume %									
Pressure	**900**	**800**	**700**	**600**	**500**	**400**	**300**	**200**	**100**
Temperature									
300	100	100	100	100	100	100	100	100	100
260	100	100	100	100	100	100	100	100	100
245	100	100	100	100	100	100	100	100	100
230	100	100	93.3273	100	100	100	100	100	100
215	100	100	62.4311	91.1553	100	100	100	100	100
200	0	0	17.9341	75.0456	93.6696	100	100	100	100
185	0	0	0	50.5445	84.1679	96.6795	100	100	100
170	0	0	0	0	70.45	91.077	99.3402	100	100
140	0	0	0	0	0	71.5811	92.3468	99.5541	100
110	0	0	0	0	0	0	78.4051	95.5766	100
80	0	0	0	0	0	0	0	88.7984	98.956
50	0	0	0	0	0	0	0	15.8146	96.994

ng									
Pressure	**900**	**800**	**700**	**600**	**500**	**400**	**300**	**200**	**100**
Temperature									
300	0.000163	0.000163	0.000163	0.000163	0.000163	0.000163	0.000163	0.000163	0.000163
260	0.000163	0.000163	0.000163	0.000163	0.000163	0.000163	0.000163	0.000163	0.000163
245	0.000163	0.000163	0.000163	0.000163	0.000163	0.000163	0.000163	0.000163	0.000163
230	0.000163	0.000163	0.000142	0.000163	0.000163	0.000163	0.000163	0.000163	0.000163
215	0.000163	0.000163	6.89E-05	0.000125	0.000163	0.000163	0.000163	0.000163	0.000163
200	0	0	1.34E-05	7.68E-05	0.000125	0.000163	0.000163	0.000163	0.000163
185	0	0	0	3.65E-05	8.59E-05	0.000133	0.000163	0.000163	0.000163
170	0	0	0	0	5.3E-05	9.82E-05	0.000153	0.000163	0.000163
140	0	0	0	0	0	4.26E-05	8.86E-05	0.000152	0.000163
110	0	0	0	0	0	0	4.18E-05	9.24E-05	0.000163
80	0	0	0	0	0	0	0	5.18E-05	0.000119
50	0	0	0	0	0	0	0	1.74E-06	7.8E-05

Vg									
Pressure	**900**	**800**	**700**	**600**	**500**	**400**	**300**	**200**	**100**
Temperature									
300	0.000883	0.000883	0.000883	0.000883	0.000883	0.000883	0.000883	0.000883	0.000883
260	0.000883	0.000883	0.000883	0.000883	0.000883	0.000883	0.000883	0.000883	0.000883
245	0.000883	0.000883	0.000883	0.000883	0.000883	0.000883	0.000883	0.000883	0.000883
230	0.000883	0.000883	0.000824	0.000883	0.000883	0.000883	0.000883	0.000883	0.000883
215	0.000883	0.000883	0.000551	0.000805	0.000883	0.000883	0.000883	0.000883	0.000883
200	0	0	0.000158	0.000663	0.000827	0.000883	0.000883	0.000883	0.000883
185	0	0	0	0.000446	0.000743	0.000853	0.000883	0.000883	0.000883
170	0	0	0	0	0.000622	0.000804	0.000877	0.000883	0.000883
140	0	0	0	0	0	0.000632	0.000815	0.000879	0.000883
110	0	0	0	0	0	0	0.000692	0.000844	0.000883
80	0	0	0	0	0	0	0	0.000784	0.000874
50	0	0	0	0	0	0	0	0.00014	0.000856

P*V/Z*n									
Pressure	**900**	**800**	**700**	**600**	**500**	**400**	**300**	**200**	**100**
Temperature									
300	8152.778	6742.261	5499.383	4411.979	3458.081	2614.072	1860.537	1181.442	564.4638
260	10747.99	8318.003	6375.21	4889.866	3713.496	2744.013	1920.192	1203.52	569.1553
245	12949.04	9745.231	7007.541	5177.688	3850.407	2808.473	1948.081	1213.509	571.1985
230	15620.27	12849.93	8311.661	5596.367	4025.165	2885.238	1980.169	1224.634	573.4388
215	17788.96	16294.64	10987.67	6776.244	4262.387	2979.387	2017.336	1237.096	575.9418
200	-	-	15779.08	8829.388	5196.455	3097.965	2061.146	1251.115	578.6524
185	-	-	-	12306.61	6651.052	3668.814	2113.211	1267.085	581.6387
170	-	-	-	-	8922.458	4621.648	2275.708	1285.451	584.9088
140	-	-	-	-	-	8250.816	3573.261	1408.493	592.7272
110	-	--	-	-	-	-	6388.822	2189.012	602.6313
80	-	-	-	-	-	-	-	3607.223	813.8506
50	-	-	-	-	-	-	-	19288.18	1213.322

APPENDIX B: Ethane – Hexane System

Z-factor for GAS							
P	**1000**	**900**	**800**	**700**	**600**	**500**	**400**
T							
400	0.5399	0.5741	0.617	0.6647	0.7144	0.7643	0.8135
370	0.4519	0.4833	0.5351	0.5981	0.6628	0.7254	0.7851
350	0.3922	0.5243	0.5782	0.6184	0.6517	0.6934	0.7627
340	0.3666	0.5467	0.5957	0.6344	0.6673	0.6956	0.7501
325	0.3354	0.5719	0.6169	0.6544	0.6872	0.7162	0.7414
310	0.3122	0.5899	0.6331	0.6702	0.7034	0.7333	0.7599
280	0	0	0.6529	0.691	0.7258	0.758	0.7877
250	0	0	0.658	0.6988	0.7365	0.7717	0.8049
220	0	0	0	0.6942	0.7362	0.7755	0.8127

Vapor Phase mol %							
P	**1000**	**900**	**800**	**700**	**600**	**500**	**400**
T							
400	100	100	100	100	100	100	100
370	100	100	100	100	100	100	100
350	100	49.452	65.3286	77.0169	89.2658	100	100
340	100	37.0256	54.4295	66.6592	78.4326	92.6828	100
325	100	24.1501	41.9613	54.4565	65.6539	77.9262	94.9498
310	100	14.1959	32.1422	44.8102	55.6721	66.7135	80.5289
280	0	0	16.0333	29.5643	40.5189	50.5241	61.1499
250	0	0	0.5125	16.2088	28.3557	38.6557	48.3666
220	0	0	0	1.5033	16.4047	28.2728	38.5036

Vapor Phase Volume %							
P	**1000**	**900**	**800**	**700**	**600**	**500**	**400**
T							
400	100	100	100	100	100	100	100
370	100	100	100	100	100	100	100
350	100	61.0977	79.9778	89.9712	96.5387	100	100
340	100	50.8061	72.9682	84.9542	92.7493	98.2505	100
325	100	38.2175	63.8549	78.3171	87.7246	94.3085	99.1312
310	100	25.7312	55.1826	72.1521	83.1602	90.7969	96.3343
280	0	0	35.1553	59.2237	74.2942	84.3873	91.4751
250	0	0	1.5177	41.3375	63.8426	77.7905	87.0104
220	0	0	0	5.4058	47.4279	69.322	82.1971

n_g							
P	**1000**	**900**	**800**	**700**	**600**	**500**	**400**
T							
400	0.00017	0.00017	0.00017	0.00017	0.00017	0.00017	0.00017
370	0.00017	0.00017	0.00017	0.00017	0.00017	0.00017	0.00017
350	0.000177	8.76E-05	0.00011	0.00013	0.00015	0.00017	0.00017
340	0.000177	6.56E-05	9.64E-05	0.000118	0.000139	0.000164	0.000177
325	0.000177	4.28E-05	7.43E-05	9.65E-05	0.000116	0.000138	0.000168
310	0.000177	2.51E-05	5.69E-05	7.94E-05	9.86E-05	0.000118	0.000143
280	0	0	2.84E-05	5.24E-05	7.18E-05	8.95E-05	0.000108
250	0	0	9.08E-07	2.87E-05	5.02E-05	6.85E-05	8.57E-05
220	0	0	0	2.66E-06	2.91E-05	5.01E-05	6.82E-05

v_g							
P	**1000**	**900**	**800**	**700**	**600**	**500**	**400**
T							
400	0.000883	0.000883	0.000883	0.000883	0.000883	0.000883	0.000883
370	0.000883	0.000883	0.000883	0.000883	0.000883	0.000883	0.000883
350	0.000883	0.000539	0.000706	0.000794	0.000852	0.000883	0.000883
340	0.000883	0.000449	0.000644	0.00075	0.000819	0.000867	0.000883
325	0.000883	0.000337	0.000564	0.000691	0.000774	0.000833	0.000875
310	0.000883	0.000227	0.000487	0.000637	0.000734	0.000802	0.00085
280	0	0	0.00031	0.000523	0.000656	0.000745	0.000808
250	0	0	1.34E-05	0.000365	0.000564	0.000687	0.000768
220	0	0	0	4.77E-05	0.000419	0.000612	0.000726

P*V/Z*n							
P	**1000**	**900**	**800**	**700**	**600**	**500**	**400**
T							
400	9229.52	7811.733	6460.963	5247.649	4185.065	3259.857	2450.162
370	11026.82	9279.363	7449.849	5831.989	4510.879	3434.669	2538.794
350	12705.3	10568.08	8440.544	6589.288	4961.492	3593.177	2613.357
340	13592.52	11256.4	8971.274	7007.322	5298.301	3796.982	2657.255
325	14856.94	12409.61	9833.609	7665.74	5813.282	4210.13	2806.83
310	15960.98	13780.14	10810.27	8380.273	6349.204	4624.215	3137.799
280	#DIV/0!	#DIV/0!	13387.63	10112.08	7553.078	5489.992	3785.286
250	#DIV/0!	#DIV/0!	17941.08	12730.07	9139.893	6497.211	4454.881
220	#DIV/0!	#DIV/0!	#DIV/0!	18068.42	11741.23	7877.4	5235.731

APPENDIX C: Ethane – Heptane System

Z-factor for GAS											
P	**1200**	**1100**	**1000**	**900**	**850**	**830**	**820**	**800**	**700**	**600**	**500**
T											
530	0.6641	0.6788	0.6973	0.7195	0.7318	0.7369	0.7395	0.7448	0.7726	0.8024	0.8337
510	0.632	0.6473	0.6673	0.6918	0.7055	0.7112	0.7141	0.72	0.7511	0.7844	0.819
490	0.5965	0.6117	0.633	0.66	0.6753	0.6817	0.685	0.6916	0.7267	0.764	0.8027
460	0.5371	0.5499	0.5715	0.6021	0.6203	0.628	0.632	0.64	0.6828	0.7281	0.7743
430	0.4743	0.4795	0.4958	0.5301	0.558	0.5672	0.5716	0.5799	0.6261	0.6829	0.7396
420	0.4541	0.4556	0.4841	0.5622	0.5849	0.5929	0.5967	0.604	0.636	0.6651	0.7262
400	0.4175	0.4111	0.5621	0.6076	0.6259	0.6327	0.636	0.6424	0.6715	0.6966	0.718
360	0.3637	0.3465	0.6267	0.6617	0.6775	0.6836	0.6865	0.6924	0.7202	0.7456	0.7687
350	0.3541	0.3354	0.636	0.6702	0.6858	0.6919	0.6948	0.7007	0.7286	0.7543	0.778

Vapor Phase Mol %											
P	**1173**	**1100**	**1000**	**900**	**850**	**830**	**820**	**800**	**700**	**600**	**500**
T											
530	100	100	100	100	100	100	100	100	100	100	100
510	100	100	100	100	100	100	100	100	100	100	100
490	100	100	100	100	100	100	100	100	100	100	100
460	100	100	100	100	100	100	100	100	100	100	100
430	100	100	100	98.2702	95.8828	96.1486	96.4208	97.1812	100	100	100
420	100	100	76.5794	74.3418	77.8164	79.2777	80.023	81.5455	90.0218	100	100
400	100	100	35.554	51.4841	56.862	58.8233	59.7766	61.6411	70.6288	80.2855	92.7156
360	100	100	15.5698	29.5651	34.9393	36.9062	37.8582	39.7072	48.1858	56.1581	64.6852
350	100	100	25.7235	35.8511	31.0876	33.0533	34.0045	44.2709	5.2421	52.0377	60.0799

Vapor Phase Volume %											
P	**1173**	**1100**	**1000**	**900**	**850**	**830**	**820**	**800**	**700**	**600**	**500**
T											
530	100	100	100	100	100	100	100	100	100	100	100
510	100	100	100	100	100	100	100	100	100	100	100
490	100	100	100	100	100	100	100	100	100	100	100
460	100	100	100	100	100	100	100	100	100	100	100
430	100	100	100	98.8335	97.8828	97.8425	98.0455	98.5371	100	100	100
420	100	100	79.0712	82.9695	86.9479	88.3747	89.023	90.3626	95.934	100	100
400	100	100	46.4463	67.7207	74.2393	76.4586	77.502	79.4715	87.5241	93.5398	98.249
360	100	100	27.0056	50.1185	58.3392	61.2147	62.5772	65.165	75.887	83.9386	90.1971
350	100	100	22.0228	46.127	54.8077	57.8519	59.2953	62.0384	73.4134	81.9477	88.5638

n_g											
P	**1173**	**1100**	**1000**	**900**	**850**	**830**	**820**	**800**	**700**	**600**	**500**
T											
530	0.00015	0.00015	0.00015	0.00015	0.00015	0.00015	0.00015	0.00015	0.00015	0.00015	0.00015
510	0.00015	0.00015	0.00015	0.00015	0.00015	0.00015	0.00015	0.00015	0.00015	0.00015	0.00015
490	0.00015	0.00015	0.00015	0.00015	0.00015	0.00015	0.00015	0.00015	0.00015	0.00015	0.00015
460	0.00015	0.00015	0.00015	0.00015	0.00015	0.00015	0.00015	0.00015	0.00015	0.00015	0.00015
430	0.00015	0.00015	0.00015	0.000147	0.000144	0.000144	0.000145	0.000146	0.00015	0.00015	0.00015
420	0.00015	0.00015	0.000115	0.000112	0.000117	0.000119	0.00012	0.000122	0.000135	0.00015	0.00015
400	0.00015	0.00015	5.33E-05	7.72E-05	8.53E-05	8.82E-05	8.97E-05	9.25E-05	0.000106	0.00012	0.000139
360	0.00015	0.00015	2.34E-05	4.43E-05	5.24E-05	5.54E-05	5.68E-05	5.96E-05	7.23E-05	8.42E-05	9.7E-05
350	0.00015	0.00015	3.86E-05	5.38E-05	4.66E-05	4.96E-05	5.1E-05	6.64E-05	7.86E-06	7.81E-05	9.01E-05

V_g											
P	**1173**	**1100**	**1000**	**900**	**850**	**830**	**820**	**800**	**700**	**600**	**500**
T											
530	0.000883	0.000883	0.000883	0.000883	0.000883	0.000883	0.000883	0.000883	0.000883	0.000883	0.000883
510	0.000883	0.000883	0.000883	0.000883	0.000883	0.000883	0.000883	0.000883	0.000883	0.000883	0.000883
490	0.000883	0.000883	0.000883	0.000883	0.000883	0.000883	0.000883	0.000883	0.000883	0.000883	0.000883
460	0.000883	0.000883	0.000883	0.000883	0.000883	0.000883	0.000883	0.000883	0.000883	0.000883	0.000883
430	0.000883	0.000883	0.000883	0.000873	0.000864	0.000864	0.000866	0.00087	0.000883	0.000883	0.000883
420	0.000883	0.000883	0.000698	0.000732	0.000768	0.00078	0.000786	0.000798	0.000847	0.000883	0.000883
400	0.000883	0.000883	0.00041	0.000598	0.000655	0.000675	0.000684	0.000702	0.000773	0.000826	0.000867
360	0.000883	0.000883	0.000238	0.000442	0.000515	0.00054	0.000552	0.000575	0.00067	0.000741	0.000796
350	0.000883	0.000883	0.000194	0.000407	0.000484	0.000511	0.000523	0.000548	0.000648	0.000723	0.000782

P*Vg/Z*ng											
P	**1173**	**1100**	**1000**	**900**	**850**	**830**	**820**	**800**	**700**	**600**	**500**
T											
530	10634.54	9537.223	8440.174	7361.779	6835.93	6628.887	6525.995	6321.518	5332.298	4400.798	3529.647
510	11174.68	10001.34	8819.621	7656.548	7090.763	6868.429	6758.12	6539.259	5484.933	4501.785	3593
490	11839.73	10583.4	9297.525	8025.455	7407.868	7165.654	7045.217	6807.789	5669.098	4621.99	3665.961
460	13149.13	11772.81	10298.05	8797.21	8064.7	7778.386	7636.034	7356.667	6033.587	4849.883	3800.422
430	14890.15	13501.29	11870.38	10049.35	9152.115	8763.902	8585.185	8232.381	6579.993	5170.889	3978.727
420	15552.52	14209.54	12552.85	10514.97	9556.444	9184.269	8997.384	8637.993	6902.984	5309.277	4052.144
400	16915.93	15747.67	13677.92	11466.85	10435.1	10035.25	9838.061	9449.233	7602.719	5906.064	4343.021
360	19418.2	18683.6	16288.54	13569.73	12328.97	11852.32	11619.85	11159.61	9008.745	7078.899	5337.917
350	19944.65	19301.93	7922.394	10168.62	12860.18	12356.87	12111.81	9416.102	79186.29	7372.196	5575.56

APPENDIX D: 40%Ethane – 50%Pentane System with Initial Pressure of 800 psi

Z-factor for GAS											
P	**800**	**750**	**700**	**650**	**600**	**550**	**500**	**450**	**400**	**350**	**300**
T											
350	0.5001	0.5332	0.5686	0.6046	0.6401	0.6748	0.7085	0.7412	0.7729	0.8037	0.8337
340	0.4586	0.4946	0.5348	0.5758	0.6159	0.6545	0.6914	0.7269	0.761	0.7939	0.8257
330	0.4113	0.4477	0.4936	0.5416	0.5879	0.6314	0.6725	0.7112	0.7481	0.7833	0.8172
320	0.3624	0.4614	0.5001	0.5289	0.5545	0.605	0.6512	0.694	0.734	0.772	0.8081
310	0.3213	0.4952	0.5271	0.5532	0.5757	0.5956	0.6269	0.6747	0.7187	0.7597	0.7983
300	0.2917	0.5207	0.5493	0.5738	0.5956	0.6151	0.6329	0.6531	0.7017	0.7463	0.7878
280	0.2558	0.247	0.5835	0.6066	0.6278	0.6473	0.6654	0.6821	0.6974	0.7156	0.7642
260	0	0	0	0.63	0.6514	0.6715	0.6903	0.708	0.7246	0.7399	0.7536
240	0	0	0	0	0.6676	0.6886	0.7084	0.7273	0.7453	0.7621	0.7778

Vapor Phase Mol %											
P	**800**	**750**	**700**	**650**	**600**	**550**	**500**	**450**	**400**	**350**	**300**
T											
350	100	100	100	100	100	100	100	100	100	100	100
340	100	100	100	100	100	100	100	100	100	100	100
330	100	100	100	100	100	100	100	100	100	100	100
320	100	58.6971	74.7971	87.6465	100	100	100	100	100	100	100
310	100	32.6658	51.08	64.8486	77.5254	90.8895	100	100	100	100	100
300	100	17.4416	35.0992	48.5823	60.5802	72.5505	85.8014	100	100	100	100
280	100	100	13.3947	26.0738	37.0515	47.3332	57.7368	69.2003	83.1937	100	100
260	0	0	0	9.9659	20.6083	30.2152	39.3909	48.73	59.0105	71.5603	89.2842
240	0	0	0	0	7.2212	16.8773	25.7394	34.2641	42.9546	52.5333	64.3386

Vapor Phase Volume %											
P	**800**	**750**	**700**	**650**	**600**	**550**	**500**	**450**	**400**	**350**	**300**
T											
350	100	100	100	100	100	100	100	100	100	100	100
340	100	100	100	100	100	100	100	100	100	100	100
330	100	100	100	100	100	100	100	100	100	100	100
320	100	68.0866	84.6406	93.9784	100	100	100	100	100	100	100
310	100	45.706	68.3432	81.6279	90.5452	96.9504	100	100	100	100	100
300	100	28.9332	54.9249	71.0466	82.0455	89.9782	95.9143	100	100	100	100
280	100	100	28.4255	50.7734	66.1517	77.2119	85.4294	91.6902	96.5565	100	100
260	0	0	0	26.1152	48.3718	63.8774	75.0849	83.4237	89.7747	94.7056	98.596
240	0	0	0	0	23.0338	46.8606	63.0541	74.5372	82.9528	89.2849	94.1526

n_g											
P	**800**	**750**	**700**	**650**	**600**	**550**	**500**	**450**	**400**	**350**	**300**
T											
350	0.000163	0.000163	0.000163	0.000163	0.000163	0.000163	0.00016256	0.000163	0.000163	0.000163	0.000163
340	0.000163	0.000163	0.000163	0.000163	0.000163	0.000163	0.00016256	0.000163	0.000163	0.000163	0.000163
330	0.000163	0.000163	0.000163	0.000163	0.000163	0.000163	0.00016256	0.000163	0.000163	0.000163	0.000163
320	0.000163	9.54E-05	0.000122	0.000142	0.000163	0.000163	0.00016256	0.000163	0.000163	0.000163	0.000163
310	0.000163	5.31E-05	8.3E-05	0.000105	0.000126	0.000148	0.00016256	0.000163	0.000163	0.000163	0.000163
300	0.000163	2.84E-05	5.71E-05	7.9E-05	9.85E-05	0.000118	0.00013948	0.000163	0.000163	0.000163	0.000163
280	0.000163	0.000163	2.18E-05	4.24E-05	6.02E-05	7.69E-05	9.3855E-05	0.000112	0.000135	0.000163	0.000163
260	0	0	0	1.62E-05	3.35E-05	4.91E-05	6.4033E-05	7.92E-05	9.59E-05	0.000116	0.000145
240	0	0	0	0	1.17E-05	2.74E-05	4.1841E-05	5.57E-05	6.98E-05	8.54E-05	0.000105

V_g											
P	**800**	**750**	**700**	**650**	**600**	**550**	**500**	**450**	**400**	**350**	**300**
T											
350	0.000883	0.000883	0.000883	0.000883	0.000883	0.000883	0.000883	0.000883	0.000883	0.000883	0.000883
340	0.000883	0.000883	0.000883	0.000883	0.000883	0.000883	0.000883	0.000883	0.000883	0.000883	0.000883
330	0.000883	0.000883	0.000883	0.000883	0.000883	0.000883	0.000883	0.000883	0.000883	0.000883	0.000883
320	0.000883	0.000601	0.000747	0.00083	0.000883	0.000883	0.000883	0.000883	0.000883	0.000883	0.000883
310	0.000883	0.000404	0.000603	0.000721	0.0008	0.000856	0.000883	0.000883	0.000883	0.000883	0.000883
300	0.000883	0.000255	0.000485	0.000627	0.000724	0.000795	0.000847	0.000883	0.000883	0.000883	0.000883
280	0.000883	0.000883	0.000251	0.000448	0.000584	0.000682	0.000754	0.00081	0.000853	0.000883	0.000883
260	0	0	0	0.000231	0.000427	0.000564	0.000663	0.000737	0.000793	0.000836	0.000871
240	0	0	0	0	0.000203	0.000414	0.000557	0.000658	0.000732	0.000788	0.000831

P*V/Z*n											
P	**800**	**750**	**700**	**650**	**600**	**550**	**500**	**450**	**400**	**350**	**300**
T											
350	8689.378	7640.587	6687.238	5839.838	5091.655	4427.343	3833.414	3297.864	2811.203	2365.537	1954.641
340	9475.705	8236.88	7109.879	6131.931	5291.717	4564.662	3928.224	3362.741	2855.163	2394.737	1973.579
330	10565.42	9099.756	7703.329	6519.14	5543.747	4731.662	4038.623	3436.975	2904.397	2427.144	1994.107
320	11991.05	10241.99	8603.809	7157.953	5877.671	4938.134	4170.722	3522.156	2960.189	2462.671	2016.563
310	13524.92	11511.08	9651.727	8033.87	6611.987	5350.563	4332.388	3622.909	3023.207	2502.543	2041.318
300	14897.35	12978.95	10832.19	8998.573	7410.99	6023.785	4797.108	3742.729	3096.45	2547.476	2068.525
280	16988.11	16493.77	13828.91	11334.4	9268.741	7528.891	6039.451	4748.265	3615.969	2656.766	2132.406
260	#DIV/0!	#DIV/0!	#DIV/0!	14686.06	11743.81	9405.763	7499.709	5910.55	4561.86	3400.589	2387.925
240	#DIV/0!	#DIV/0!	#DIV/0!	#DIV/0!	15572.08	12046.37	9392.083	7311.193	5629.967	4239.894	3065.982

APPENDIX E: 40%Ethane – 50%Pentane System with Initial Pressure of 600 psi

Z-factor for GAS							
P	**600**	**550**	**500**	**450**	**400**	**350**	**300**
T							
350	0.6401	0.6748	0.7085	0.7412	0.7729	0.8037	0.8337
340	0.6159	0.6545	0.6914	0.7269	0.761	0.7939	0.8257
330	0.5879	0.6314	0.6725	0.7112	0.7481	0.7833	0.8172
320	0.5545	0.605	0.6512	0.694	0.734	0.772	0.8081
310	0.5757	0.5956	0.6269	0.6747	0.7187	0.7597	0.7983
300	0.5956	0.6151	0.6329	0.6531	0.7017	0.7463	0.7878
280	0.6278	0.6473	0.6654	0.6821	0.6974	0.7156	0.7642
260	0.6514	0.6715	0.6903	0.708	0.7246	0.7399	0.7536
240	0.6676	0.6886	0.7084	0.7273	0.7453	0.7621	0.7778

Vapor Phase Mol %							
P	**600**	**550**	**500**	**450**	**400**	**350**	**300**
T							
350	100	100	100	100	100	100	100
340	100	100	100	100	100	100	100
330	100	100	100	100	100	100	100
320	100	100	100	100	100	100	100
310	77.5254	90.8895	100	100	100	100	100
300	60.5802	72.5505	85.8014	100	100	100	100
280	37.0515	47.3332	57.7368	69.2003	83.1937	100	100
260	20.6083	30.2152	39.3909	48.73	59.0105	71.5603	89.2842
240	7.2212	16.8773	25.7394	34.2641	42.9546	52.5333	64.3386

Vapor Phase Volume %							
P	**600**	**550**	**500**	**450**	**400**	**350**	**300**
T							
350	100	100	100	100	100	100	100
340	100	100	100	100	100	100	100
330	100	100	100	100	100	100	100
320	100	100	100	100	100	100	100
310	90.5452	96.9504	100	100	100	100	100
300	82.0455	89.9782	95.9143	100	100	100	100
280	66.1517	77.2119	85.4294	91.6902	96.5565	100	100
260	48.3718	63.8774	75.0849	83.4237	89.7747	94.7056	98.596
240	23.0338	46.8606	63.0541	74.5372	82.9528	89.2849	94.1526

n_g							
Pressure	**600**	**550**	**500**	**450**	**400**	**350**	**300**
Temperature							
350	9.53E-05	9.53E-05	9.53E-05	9.53E-05	9.53E-05	9.53E-05	9.5252E-05
340	9.53E-05	9.53E-05	9.53E-05	9.53E-05	9.53E-05	9.53E-05	9.5252E-05
330	9.53E-05	9.53E-05	9.53E-05	9.53E-05	9.53E-05	9.53E-05	9.5252E-05
320	9.53E-05	9.53E-05	9.53E-05	9.53E-05	9.53E-05	9.53E-05	9.5252E-05
310	7.38E-05	8.66E-05	9.53E-05	9.53E-05	9.53E-05	9.53E-05	9.5252E-05
300	5.77E-05	6.91E-05	8.17E-05	9.53E-05	9.53E-05	9.53E-05	9.5252E-05
280	3.53E-05	4.51E-05	5.5E-05	6.59E-05	7.92E-05	9.53E-05	9.5252E-05
260	1.96E-05	2.88E-05	3.75E-05	4.64E-05	5.62E-05	6.82E-05	8.5045E-05
240	6.88E-06	1.61E-05	2.45E-05	3.26E-05	4.09E-05	5E-05	6.1284E-05

V_g							
Pressure	**600**	**550**	**500**	**450**	**400**	**350**	**300**
Temperature							
350	0.000883	0.000883	0.000883	0.000883	0.000883	0.000883	0.000883
340	0.000883	0.000883	0.000883	0.000883	0.000883	0.000883	0.000883
330	0.000883	0.000883	0.000883	0.000883	0.000883	0.000883	0.000883
320	0.000883	0.000883	0.000883	0.000883	0.000883	0.000883	0.000883
310	0.0008	0.000856	0.000883	0.000883	0.000883	0.000883	0.000883
300	0.000724	0.000795	0.000847	0.000883	0.000883	0.000883	0.000883
280	0.000584	0.000682	0.000754	0.00081	0.000853	0.000883	0.000883
260	0.000427	0.000564	0.000663	0.000737	0.000793	0.000836	0.000871
240	0.000203	0.000414	0.000557	0.000658	0.000732	0.000788	0.000831